

# The effect of breached relay ramp structures on deep-lacustrine sedimentary systems

Gayle E. Plenderleith  | Thomas J. H. Dodd  | Dave J. McCarthy

British Geological Survey, The Lyell Centre, Edinburgh, UK

## Correspondence

Gayle E. Plenderleith, British Geological Survey, The Lyell Centre, Research Avenue South, Edinburgh EH144AP, UK.  
Email: gaylep@bgs.ac.uk

## Abstract

Fault relay ramps are important sediment delivery points along rift margins and often provide persistent flow pathways in deepwater sedimentary basins. They form as tilted rock volumes between en-echelon fault segments, which become modified through progressive deformation, and may develop through-going faults that ‘breach’ the relay ramp. It is well established that hinterland drainage (fluvial/alluvial systems) is greatly affected by the presence of relay ramps at basin margins. However, the impact on deepwater (deep-marine/lacustrine) subaqueous sediment gravity flow processes, particularly by breached relay ramps, is less well documented. To better evaluate the complex geology of breached relay settings, this study examines a suite of high-quality subsurface data from the Early Cretaceous deep-lacustrine North Falkland Basin (NFB). The Isobel Embayment breached relay-ramp, an ideal example, formed during the syn-rift and was later covered by a thick transitional and early post-rift succession. Major transitional and early post-rift fan systems are observed to have consistently entered the basin at the breached relay location, directed through a significant palaeo-bathymetric low associated with the lower, abandoned ramp of the structure. More minor systems also entered the basin across the structure-bounding fault to the north. Reactivation of basin-bounding faults is shown by the introduction of new point sources along its extent. This study shows the prolonged influence of margin-located relay ramps on sedimentary systems from syn-rift, transitional and into the early post-rift phase. It suggests that these structures can become reactivated during post-rift times, providing continued control on deposition and sourcing of overlying sedimentary systems. Importantly, breached relays exert control on fan distribution, characterised by laterally extensive lobes sourced by widespread feeder systems, and hanging walls settings by small-scale lobes, with small, often line-sourced feeders. Further characterising the likely sandstone distribution in these structurally complex settings is important as these systems often form attractive hydrocarbon reservoirs.

This is an open access article under the terms of the Creative Commons Attribution License, which permits use, distribution and reproduction in any medium, provided the original work is properly cited.

© 2022 British Geological Survey. *Basin Research* published by International Association of Sedimentologists and European Association of Geoscientists and Engineers and John Wiley & Sons Ltd.

## KEYWORDS

breached relay ramp, deep-lacustrine sedimentary system, Early Cretaceous, North Falkland Basin

## 1 | INTRODUCTION

Fault relay ramps are important sediment delivery points along rift margins and often serve as persistent flow pathways in deepwater sedimentary basins (Athmer & Luthi, 2011; Bruhn & Vagle, 2005; Crossley, 1984; Gawthorpe & Hurst, 1993; Jackson & Leeder, 1994; Wells et al., 1999; Young et al., 2000; and references therein; Barret et al., 2020; Elliott et al., 2017; Hemelsdaël & Ford, 2016; Henstra et al., 2016; Serck & Braathen, 2019; Zhang & Scholz, 2015). Relay structures initially comprise a tilted or deformed volume of rock (the ramp) that forms between two overlapping, en-echelon normal faults of comparable dips. As these areas develop in response to continued fault movement, relay ramps experience fracturing, which propagates perpendicularly across the ramp and connects the overlapping fault segments. With further deformation, the relay ramp becomes breached by faults, resulting in a through-going hard-linked fault system (Childs et al., 1995; Fossen & Rotevatn, 2015; Peacock & Sanderson, 1991, 1994; Walsh et al., 1999; Figure 1).

The interaction of sediment transportation with relay ramps has long been an area of interest, as these structures are considered to strongly influence the distribution of reservoir facies in rift basin settings (Athmer et al., 2010; Carmona et al., 2016; Crossley, 1984; Gawthorpe & Colella, 1990; Gawthorpe & Hurst, 1993; Ge et al., 2018; Jackson & Leeder, 1994; Kim & Paola, 2007; Leeder & Gawthorpe, 1987; Serck & Braathen, 2019). In sub-aerial settings, the behaviour of flows within fluvial settings in developing rift systems is generally well understood (Figure 1; Commins et al., 2005; Frostick & Reid, 1989; Jackson & Leeder, 1994; Trudgill, 2002; Young et al., 2000), with a combination of outcrop studies, subsurface data sets (e.g. seismic and core data; Hemelsdaël & Ford, 2016) and numerical modelling to support these conclusions (Cowie et al., 2006).

In the sub-aqueous setting (marine or lacustrine), the effect of relay ramps on sub-aqueous sediment gravity flows has been studied using numerical modelling techniques (Athmer et al., 2010; Athmer & Luthi, 2011; Carmona et al., 2016; Ge et al., 2018; Zhang et al., 2020), through the analysis of seismic data (Barret et al., 2020; Bruhn & Vagle, 2005; Fugelli & Olsen, 2007; Gawthorpe & Hurst, 1993; Serck & Braathen, 2019; Soreghan et al., 1999), and in outcrop (Henstra et al., 2016). Previous studies have focused on understanding syn-rift subaqueous gravity flows in early-stage relay ramp configurations

### Highlights

- Early post-rift deposition associated with breached relay structures divided into two sets of systems.
  - (1) Breached relay systems where a high-proportion of the sedimentation occurs via the lower abandoned ramp.
  - (2) Hangingwall systems that enter across the bounding faults.
- Accommodation drivers (faulting to overall basin subsidence) and localised fault reactivation control overall fan geometry in both systems.
- Differential subsidence and/or localised fault reactivation affect the breached relay and hangingwall feeder system type and/or distribution.

(Athmer et al., 2010; Athmer & Luthi, 2011; Bruhn & Vagle, 2005; Fugelli & Olsen, 2007; Gawthorpe & Hurst, 1993; Kim & Paola, 2007) and suggest that the structural influence may have limited effect on syn-rift sub-aqueous gravity flow and deposition. Other studies show (mainly through numerical modelling) that large volumes of sediment are transported directly down the fault slopes (Athmer et al., 2010; Athmer & Luthi, 2011; Ge et al., 2018; Soreghan et al., 1999). A proportion of the turbidity current may be directed down the relay ramp, particularly where there are pre-existing channels present on the ramp, or where the ramp is landward tilting (Athmer et al., 2010; Athmer & Luthi, 2011). The most significant sediment accumulation occurred adjacent to bounding faults, with comparatively less at the foot of the relay ramp and limited deposition on the relay ramp itself, directly affecting the distribution of reservoir facies (Athmer et al., 2010; Athmer & Luthi, 2011; Ge et al., 2018). A study based on seismic reflection data (Fugelli & Olsen, 2007), conducted in a comparable structural setting (soft-linked relay ramps), exhibits similar turbidite geometries with those produced in numerical models (Ge et al., 2018). A larger (compared with the size of incoming flows) and more advanced relay ramp, with greater displacement, may cause redirection of the turbidity current, which can lead to increased deposition at

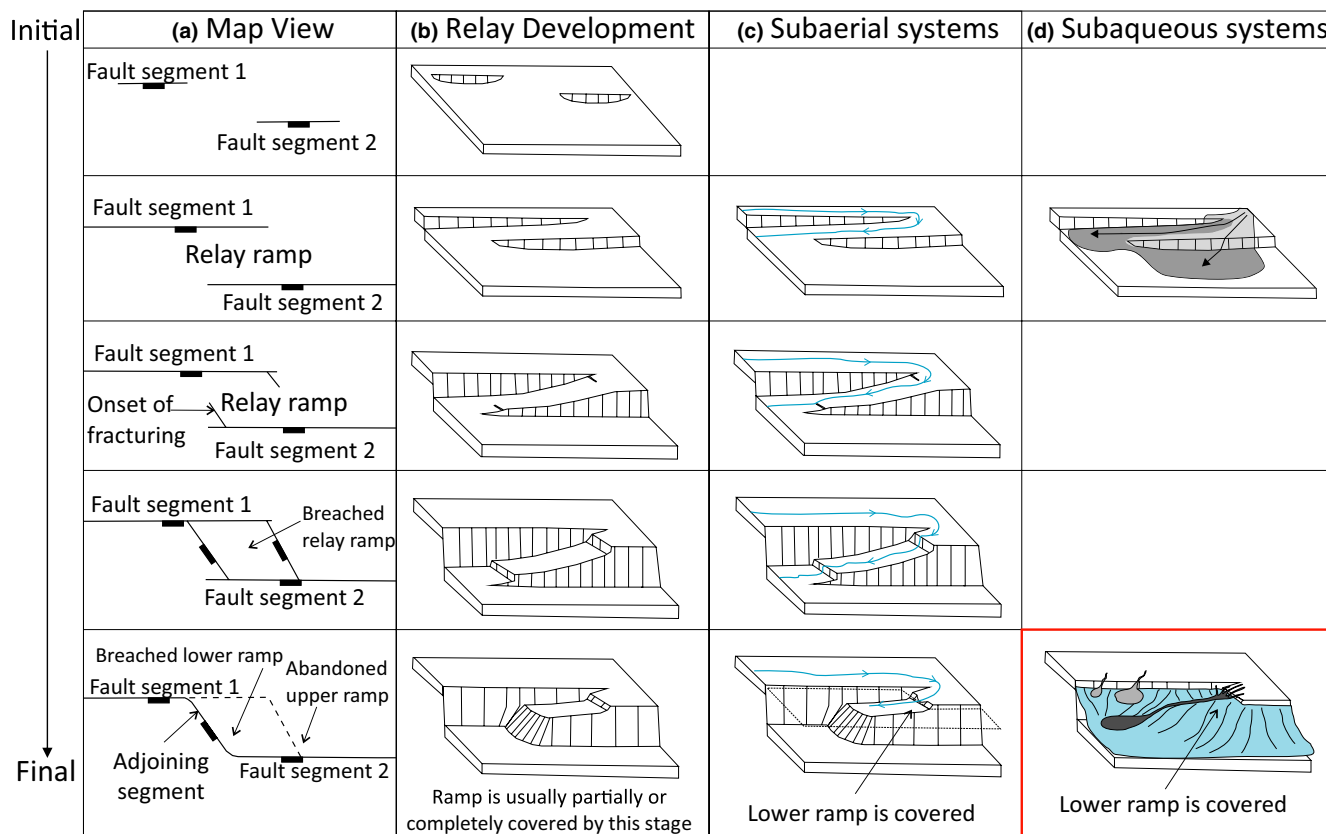


**FIGURE 1** Relay ramp development (modified after Çiftçi & Bozkurt, 2007; Peacock & Sanderson, 1994). (a) Map view of the stages of relay structure development. (b) 3D expression of the stages of relay structure development. (c) Subaerial sedimentary systems have been observed to exploit relay structures as sediment pathways into basins (modified from Trudgill, 2002). (d) Subaqueous systems do not appear to exclusively exploit early-stage relay ramps, with a significant proportion of sediment depositing directly over the fault hanging walls. The interaction of relay ramps and subaqueous deposition highlights the limited studies on the effects of advanced-stage relay ramp on subaqueous deposition (based on Athmer et al., 2010; Ge et al., 2018). The final, breached relay ramp and subaqueous sedimentary system interaction, outlined in a red box, is proposed by this study

the base of the relay ramp relative to the hanging wall area of the fault system (Ge et al., 2018).

Previous studies of subaqueous gravity flow and relay ramp interaction have focussed on syn-rift sedimentation in early-stage relay ramp settings (Athmer et al., 2010; Carmona et al., 2016; Fugelli & Olsen, 2007; Ge et al., 2018; Henstra et al., 2016; Zhang et al., 2020). However, much is left to be understood about the impact of breached relay structures on subaqueous flows during transitional and (early) post-rift phases. Furthermore, because the large proportion of rift-related deformation associated with ramp-development has ceased by the (early) post-rift, an upwards-diminishing influence of local structure on subsequent sedimentary systems might normally be expected as ramps become covered by sediments, and palaeo-topography is smoothed out (Gawthorpe & Hurst, 1993; Lambiasi & Bosworth, 1995).

Sub-aqueous sediment gravity flows transport large volumes of sediment, commonly characterised by high proportions of sand, into generally mud-prone

deep-marine settings (e.g. Bouma, 2000; Heller & Dickinson, 1985; Mutti & Normark, 1987, 1991; Richard et al., 1998; Talling, 2013), and have been shown to have the potential to deposit excellent reservoir-quality sandstones in deep-lacustrine settings (Dodd et al., 2019; Yang et al., 2019, 2020). The scale geometry and internal character of deepwater fans can also be used to infer structural information, with different fan systems developing in response to a particular set of characteristics, such as recent fault activity or changes in regional hinterland drainage patterns (Bowman, 1985; Richard et al., 1998). Where present in the system, structural influence will typically control the reservoir quality and architecture (Richard & Bowman, 1998).

To provide insight into these complex settings, this study examines an offshore subsurface data set from the North Falkland Basin (NFB) in the Falkland Islands (Figure 2). 3D seismic data have been used to map and define the key structural elements of the relay ramp located at the Isobel Embayment, while amplitude extraction

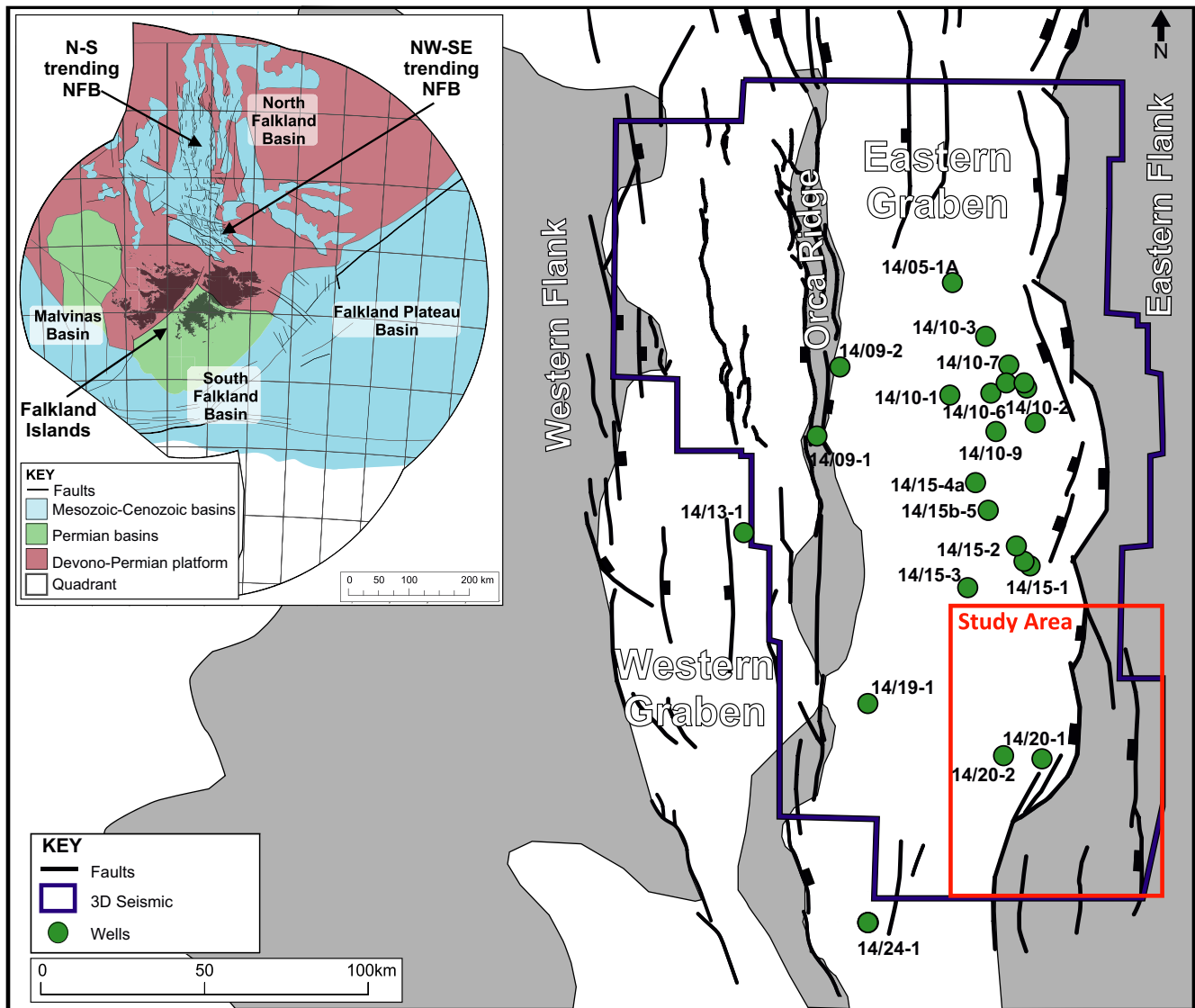


**FIGURE 2** Regional setting of the study area in the N-S trending, extensional, North Falkland Basin and the locations of wells and 3D seismic coverage

maps are used to observe, interpret and characterise the various sedimentary systems that interact with the structure. Where possible, well data have been used to support the seismic-based interpretations. This study will answer the following key questions:

- (i) How does a partially covered, breached relay ramp influence transitional and early post-rift sub-aqueous sediment gravity flows and their resultant deposits?
- (ii) What is the spatial and stratigraphic distribution of transitional and early post-rift turbidite fans preserved in a partially covered, breached relay ramp of a deep-lacustrine rift basin?
- (iii) How do transitional and early post-rift sedimentary systems at breached relay ramp locations compare with syn-rift sedimentary systems at early-stage relay ramps?
- (iv) What are the key implications for predicting sandstone distribution and potential reservoir quality in these complex settings?

Through providing case examples from the NFB, this study offers insight into transitional and early post-rift turbidite fan systems at breached relay ramps on rift margins. The findings illustrate the effects of progressive basin subsidence on hydrocarbon prospectivity and comments on clastic reservoir distribution in post-rift deep-lacustrine settings.

## 2 | REGIONAL SETTING

The NFB is an extensional, deep-lacustrine basin located 40 km north of the Falkland Islands (Figure 2). The NFB has two main structural trends; an N-S trend dominant

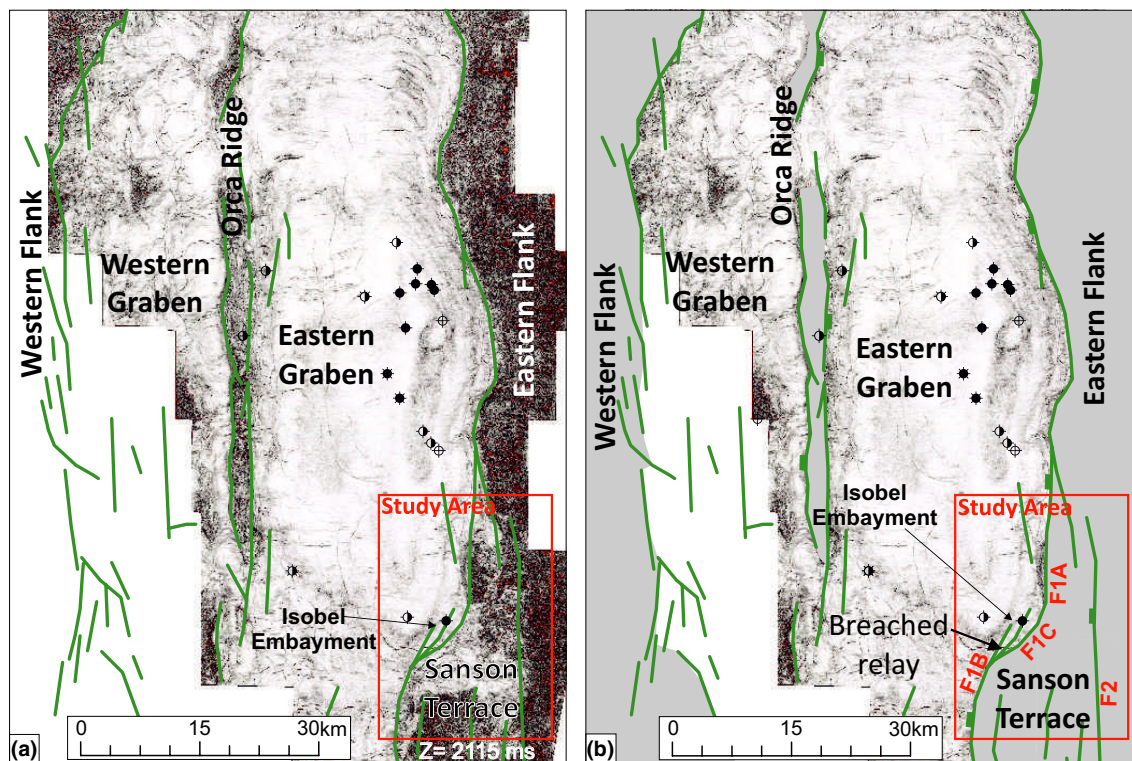


**FIGURE 3** Northern extent of the North Falkland Basin (NFB) dominated by N–S trending faults. (a) Coherency time slice at 2115 ms shows major N–S trending basement structures to the east and within the basin. Another basement high is indicated by the response in the NW corner, although much of this region is not covered the 3D seismic volume (b) The structure of the NFB is overlain on the coherency time slice at 2115 ms and shows a more complete interpretation of the basin, based on 2D seismic lines out with the 3D seismic coverage. The study area is shown to contain a major basement structure on the Eastern Flank; a breached relay ramp represented by Faults 1A–C (Fault 1A = F1A). The Sanson Terrace is situated between, and was developed by, the interaction of Faults 1A–C and 2

in the north, and a NW–SE trend dominant to the south (Figure 2). The NW–SE lineaments are thought to have developed first due to Jurassic rifting. The N–S trend developed later during the Early Cretaceous extension (Lohr & Underhill, 2015; Richards et al., 1996), which was followed by a transitional phase and a well-established post-rift phase (Richards et al., 1996). Basin subsidence was interrupted by periods of minor inversion in the Early Cretaceous (Richards et al., 1996). The depositional environment changes from fluvio-lacustrine during the active rifting phase, to marine during the basin sag phase (Richards & Hillier, 2000a). Well log and core sample analysis and seismic amplitude mapping have identified turbidite fans sourced from the basin margins in the Eastern Graben of the NFB, throughout the syn-rift to early post-rift intervals (Dodd et al., 2019; Richards et al., 2006; Richards & Hillier, 2000a).

The Eastern Graben is an N–S trending, asymmetric graben that typically characterises the northern extent of the NFB (Figures 3 and 4). It is bound by major normal faults on its eastern margin that extend N–S for up to 130 km (Figures 3 and 4). A shallower depocentre lies to

the west, referred to as the Western Graben, and is separated from the Eastern Graben by the intra-basinal high known as the ‘Orca Ridge’ (Figures 3 and 4). The Isobel Embayment, located at a large westward step in the eastern margin of the Eastern Graben, is associated with a breached relay structure and represents an important site of sediment input into the NFB throughout the syn-rift and early post-rift phases (Figure 3; Lohr & Underhill, 2015). The interaction of the basin margin faults and another major normal fault further east has led to the formation of the Sanson Terrace, situated up-dip from the Isobel Embayment in the study area (Figure 3).

## 2.1 | Tectono-stratigraphy

A model for the tectono-stratigraphy of the NFB has been defined by Richards and Hillier (2000a) using well data and regional seismic reflectors. The eight tectono-stratigraphic units identified are: pre-rift/basement; early syn-rift; late syn-rift; transitional/sag; early post-rift; middle post-rift; late post-rift and a post-uplift sag phase

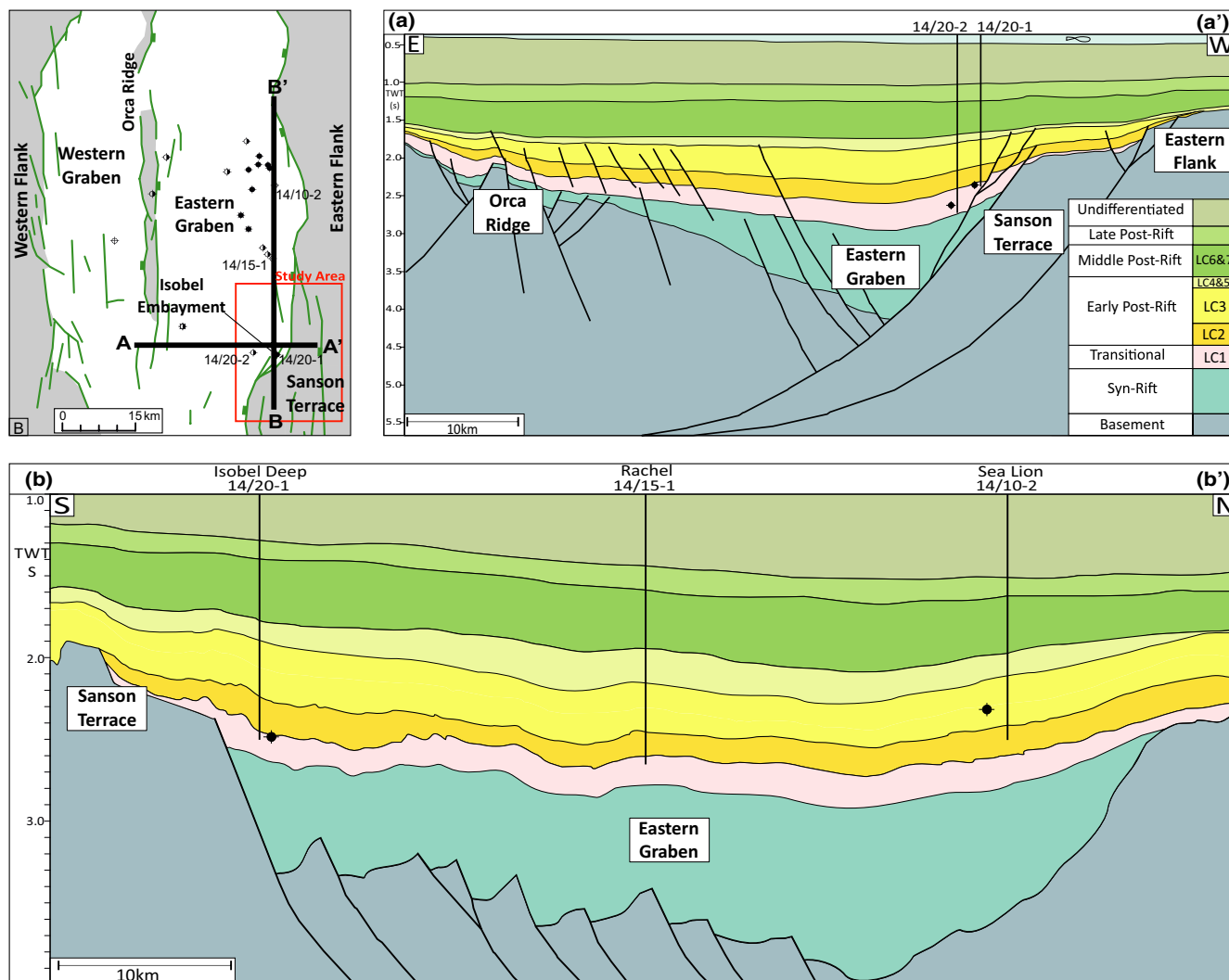


**FIGURE 4** Type sections of the North Falkland Basin and the study area. (a–a') E–W trending geo-seismic line through the Isobel Embayment showing the typically a-symmetric Eastern Graben and the locations of wells 14/20-1 and 14/20-2, which intersected the Isobel and Isobel Deep discoveries. (b–b') N–S trending line extending from the Sea Lion discovery in the north to the Isobel discoveries in the south

(Figure 6; Richards & Hillier, 2000a). The transitional to Late Post-Rift Units are further divided into sub-units, as follows: LC1 is assigned to the transitional phase; LC2 to LC5 is assigned to the early post-rift; LC6 and LC7 to the Middle Post-Rift; and L/UC1 in the Late Post-Rift, where 'LC' is Lower/Early Cretaceous and 'UC' is Upper/Late Cretaceous (Figure 6).

The pre-rift basement has been encountered in only one well in the NFB (14/09-1), located on the Orca Ridge (Figure 2). The well intersected approximately 50 m of pre-rift interpreted as Devonian to Jurassic meta-sedimentary lithologies, although some uncertainty remains due to limited data (Richards & Hillier, 2000a).

Active rifting of the NFB persisted from the Jurassic until the Early Cretaceous (Richards & Fannin, 1997). An early to late syn-rift succession was deposited in a fluvial to lacustrine environment and is comprised of

mainly conglomerates, sandstones, organic-rich claystones and reworked tuffs (Richards & Hillier, 2000a). The following transitional phase (LC1) is characterised by the deposition of lacustrine, organic-rich claystones and interbedded sandstones sourced from the basin margins (Richards et al., 1996; Richards & Hillier, 2000a).

During the early post-rift phase, extensive organic-rich, lacustrine claystones and interbedded sandstones were deposited in the Eastern Graben (Richards & Hillier, 2000a). Deltaic sandstones were deposited from the northernmost portion of the NFB, prograding southwards along the axis of the Eastern Graben. Contemporaneously, turbidity current-derived sandstones were sourced from the basin margins, fed by feeder systems (some of which were extensive) that existed up the margins at the time (Dodd et al., 2019). These turbidite fan systems developed

a complex succession of sandstones and interbedded claystone facies (Dodd et al., 2019). The eastern-derived systems are of particular importance as they typically act as the primary reservoir units for discovered hydrocarbons (e.g. Sea Lion, Isobel and Isobel Deep) in the NFB. The organic-rich claystones (up to 7.5% total organic content) deposited mainly in the early post-rift lacustrine succession, provide the source rock and sealing lithologies for the NFB (Richards & Hillier, 2000b).

The Middle Post-Rift is characterised by a transition from a lacustrine to a terrestrial-fluvial succession of sandstones, conglomerates, claystones and lignite (Richards & Hillier, 2000a). The Late Post-Rift interval contains alternating sandstones and claystones deposited in a marginal-marine to marine setting (Richards et al., 1996; Richards & Hillier, 2000a).

### 3 | DATA AND METHODS

#### 3.1 | Seismic data and analysis

About 4500 km<sup>2</sup> of 3D seismic data was acquired over the northern portion of the NFB from 2007 to 2011 (Figure 2). In 2012, three of the seismic surveys collected during this time, along with the acquisition of additional data, were subsequently merged to form a single seismic volume. The merged, full-stack, 3D seismic volume has had Kirchhoff, pre-stack time migration and spectral broadening applied; the polarity is set to zero phase European (SEG reversed polarity) throughout the volume. These merged 3D seismic data have a dominant frequency of 18 Hz and a bandwidth of 38 Hz.

Using this data set, the basin-margin structure, faulting and character have been interpreted, alongside the broad stratigraphy for the Isobel Embayment area of the NFB, providing a core structural and stratigraphic framework. This study analyses the transitional and lower part of the early post-rift succession deposited in this location, which contains the key seismic Horizons A, B, C and D used in this project. Seismic amplitude maps have been generated from a root mean square (RMS) amplitude interval of 20 ms (10 ms above and below horizon) for each interpreted horizon.

A seismo-geomorphological analysis and interpretation has been completed on this stratigraphic interval in the Isobel Embayment, which focusses on a series of well-imaged fan systems and internal lobes, identified on, along, and across the complex relay-ramp structure. The sediment sources, feeder systems and their pathways, distribution of related fan and lobe geometries, and their internal character have been documented. The interpretations of basin margin structure and sedimentary systems

are compared and analysed to assess the potential relationship(s) and controls on deposition in sub-aqueous rift settings.

#### 3.2 | Well data and analysis

Two wells, 14/20-1 and 14/20-2 (Figures 4 and 5), both situated in the Isobel Embayment are included in this study. Both these wells were drilled to test for hydrocarbons in the Isobel Complex. Well 14/20-1 was drilled in 2015 to a depth of 2526.2 m true vertical depth sub-sea (TVDss), where the well terminates in the transitional interval. Well 14/20-2 was completed in 2016 to a depth of 2987.6 m TDVss and terminates near the base of the transitional unit.

This study analyses the gamma ray (GR) wireline data within these wells (Figure 5). These wells are included to support the seismic-based interpretations made; to date, no well data are available on the Sanson Terrace.

### 4 | RESULTS AND INTERPRETATION

#### 4.1 | Structural and stratigraphic framework

##### 4.1.1 | Description

The Isobel Embayment lies on the Eastern Flank of the NFB and is bound by two N-S oriented fault segments, referred to as Fault 1A and 1B, which are connected by a NE-SW oriented Fault 1C (Figures 3 and 7). These major fault segments form the composite and through-going 'Fault 1' that displaces the basement by up to 2.0 s two-way travel time (TWTT) and which sharply divides the deep depocentre (Eastern Graben) to the west and the Sanson Terrace to the east (Figure 7b). A major sub N-S trending fault, east of the Sanson Terrace (Fault 2) is observed to offset the basement by ca. 1.0 s TWTT, separating the terrace from the Eastern Flank. Additionally, there are minor faults that interact with the basement on the Sanson Terrace, creating small (ca. <5 km wide) asymmetric grabens, most likely filled with syn-rift sediments (Figure 7b). The basement faults propagate upwards through, and terminate within the early post-rift succession, displacing it by up to 0.2 s TWTT (Figure 8). There are other relatively minor faults contained within the early post-rift on the Sanson Terrace, which trend mostly NE-SW and dominantly dip to the NE (Figure 7). They carry up to 0.04 s TWTT displacement and are less than 5 km in length—significantly smaller scale than the basement faults.

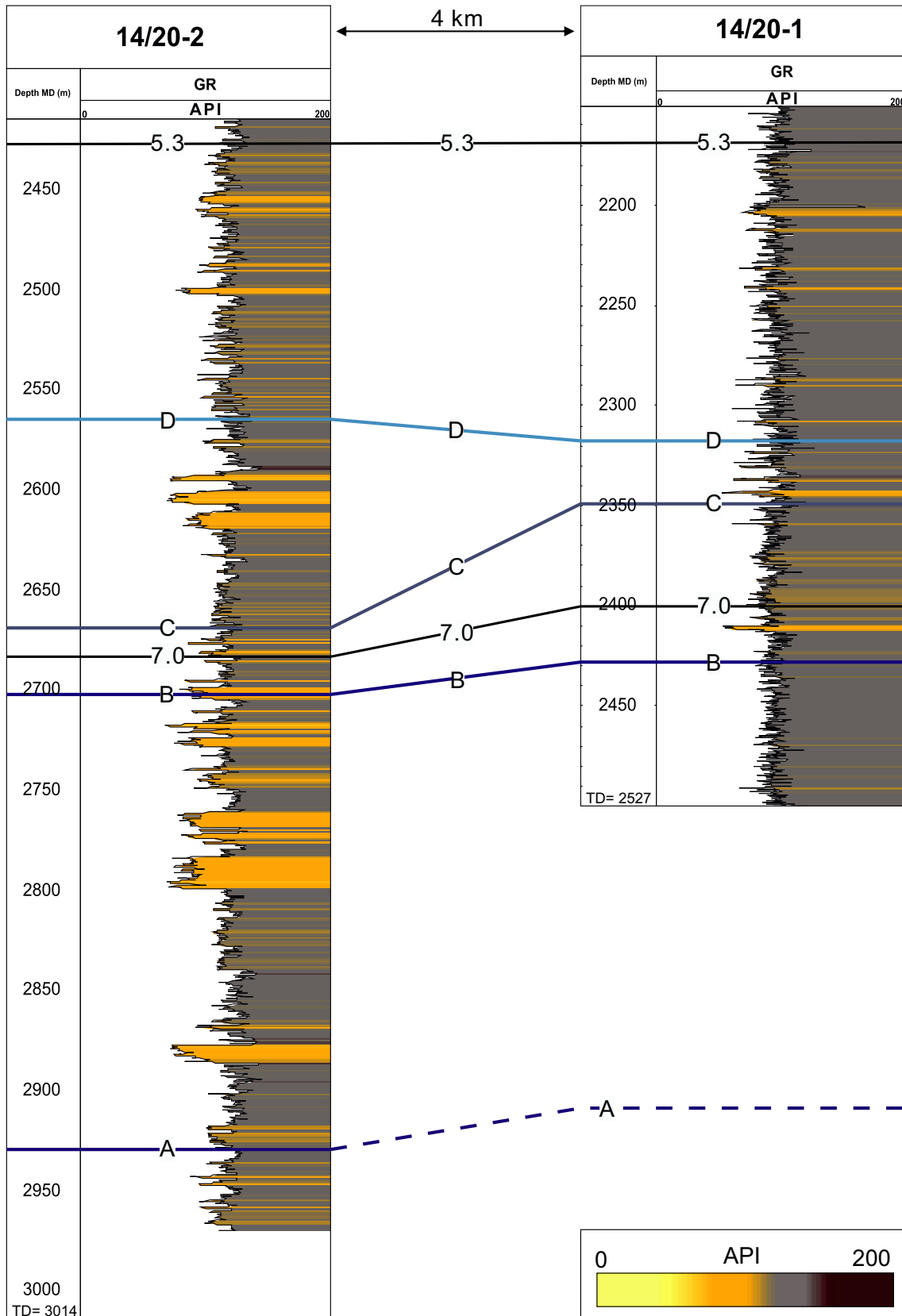


FIGURE 5 Gamma ray response in wells 14/20-1 and 14/20-2 for the study intervals, showing the positions of Horizons A-D and seismic reflectors 5.3 and 7.0

**FIGURE 6** Tectonostratigraphy of the North Falkland Basin based on Richards and Hillier (2000a) and the relative position of key Horizons A–D in the transitional and early post-rift phases. Red text denotes units that were not formalised in Richards and Hillier (2000a)

Period	Epoch	Richards and Hillier, 2000a Tectono-stratigraphy		Seismic Horizons	Study Horizons	
Paleogene	Paleocene	Post-Uplift				
Cretaceous	Upper	Late Post-Rift	L/UC1			
	Lower	Middle Post-Rift	LC6 & LC7	5.0		
		Early Post-Rift		LC4 & LC5		
				LC3	5.3	
				LC2		D
		Transitional Unit	LC1	7.0	C	
		7.25	B			
?Jurassic	Upper	Late Syn-Rift	J2		A	
		Early Syn-Rift	J1	9.0		
Devonian		Meta-Sedimentary Basement				

The syn-rift succession thickens eastwards towards Faults 1 and 2 and towards the south in the Eastern Graben and on the Sanson Terrace (Figure 8). The transitional unit thins significantly onto the Sanson Terrace (Figure 8). Horizon A is the deepest study horizon lying slightly above the base of LC1, and has been displaced up to 0.2 s TWTT by normal faults on the basin margin (Figure 8). Horizon B is located in the upper part of LC1, underlying the top of the unit which is defined by seismic reflector 7.0 (Figure 8). It has been displaced by up to 0.07 s TWTT by basin margin faults, and up to 0.04 s TWTT by minor faults on the Sanson Terrace (Figure 8).

The early post-rift, composed of the LC2, LC3, and LC4 and LC5 sub-units, is thickest in the Eastern Graben and thins onto the Sanson Terrace (and more-generally the Eastern Flank). Much of the thickness variation is accommodated by the LC3 and LC4 and LC5 sub-units, while LC2 is comparatively consistent across both the Sanson Terrace, and into the Eastern Graben. Two key seismic events or horizons have been picked and interpreted within LC2: Horizon C and Horizon D (Figures 6 and 8). Horizon C closely overlies the base of LC2 (Figure 6), and has experienced similar faulting as Horizon B. Horizon D, situated in the middle of LC2, has experienced up to 0.05 s TWTT displacement across the basin margin faults, and is displaced up to 0.02 s TWTT by minor faults on the Sanson Terrace.

### Interpretation

Up to 2.0 s TWTT of normal displacement at the top syn-rift surface on the faulted margin created an area of significantly increased accommodation space—the Isobel Embayment. The faulted margin, in conjunction with the major fault to the east, developed the Sanson Terrace. The basin margin at this location is observed to be a through-going fault system, which has interacted at depth, suggesting that the relay system has been ‘fully breached’ and reached the final stage of relay ramp development (Figure 1; Figure 7a). The basement high, located on the SW of the Sanson Terrace, is likely the upper portion of the abandoned relay ramp, with its lower counterpart covered by sediment accumulation (Figure 7). The shallower faults, of generally smaller displacement (up to 0.05 s TWTT), present on the Sanson Terrace may be associated with compaction or continued subsidence. It is possible that the minor faults were initiated as a result of movement on basement faults during the transitional and early post-rift.

## 4.2 | Tectono-stratigraphy

### 4.2.1 | Horizon A

#### Description

Horizon A is located in the lower part of the LC1 sub-unit (Figure 8). It has experienced normal faulting across the

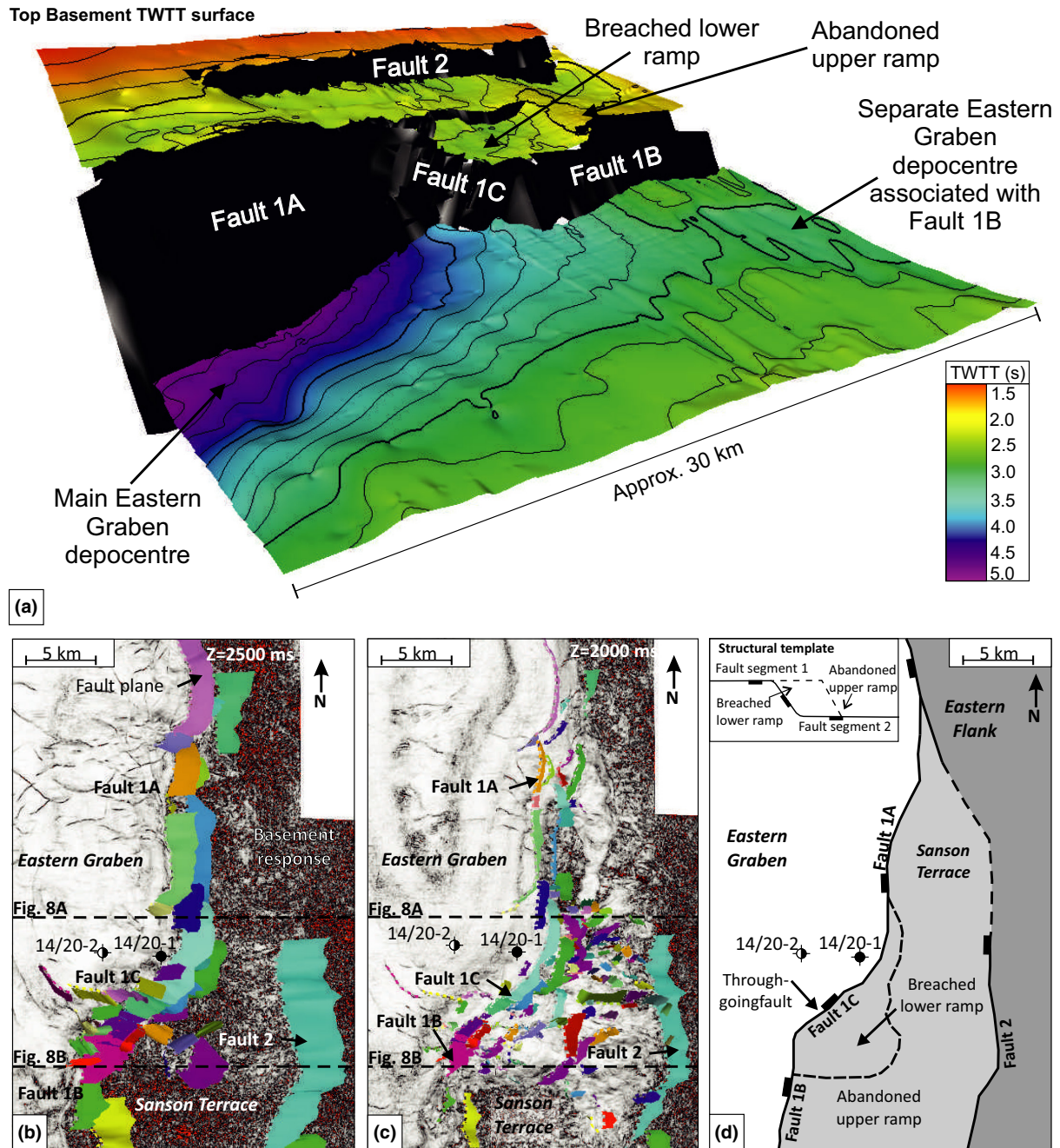


**FIGURE 7** Structural arrangement of the study area. (a) 3D view of the top Basement surface and the breached relay structure at the Isobel Embayment. (b) Time slice taken through 2500 ms shows the basement and Sanson Terrace to the east and the Eastern Graben to the west, separated by the major Fault 1 structures; Fault 1A is the northern N-S segment; Fault 1B is the southern N-S segment; Fault 1C is the NE-SW breached fault segment that hard-links the two. There are concentric faults in the Eastern Graben and a few faults on the Sanson Terrace itself. (c) Time slice at 2000 ms shows that the major Fault 1 and 2 structures remain prominent at this level. The basement response is observed only to the far east and in the SW of the Sanson Terrace. There is an increase of faults at this shallower level, over the Sanson Terrace; the dominant trend is NE-SW. (d) Proposed structural arrangement of the study area, showing the main through-going, basin bounding Fault 1 and the suspected location of the buried and abandoned, breached relay ramp outlined by the dotted line

basin margin (Fault 1), leading to a sharp change in topography along its length (Figure 9a). The time-structure map (Figure 9a) shows the Eastern Graben trending N-S along Fault 1A, into the Isobel Embayment at Fault 1C located

on the Sanson Terrace. A major, NW-SE trending palaeobathymetric low, up to 10 km in width, extends across the terrace from the major fault that bounds the terrace to the east (Fault 2) to the NW limits of the Isobel Embayment.

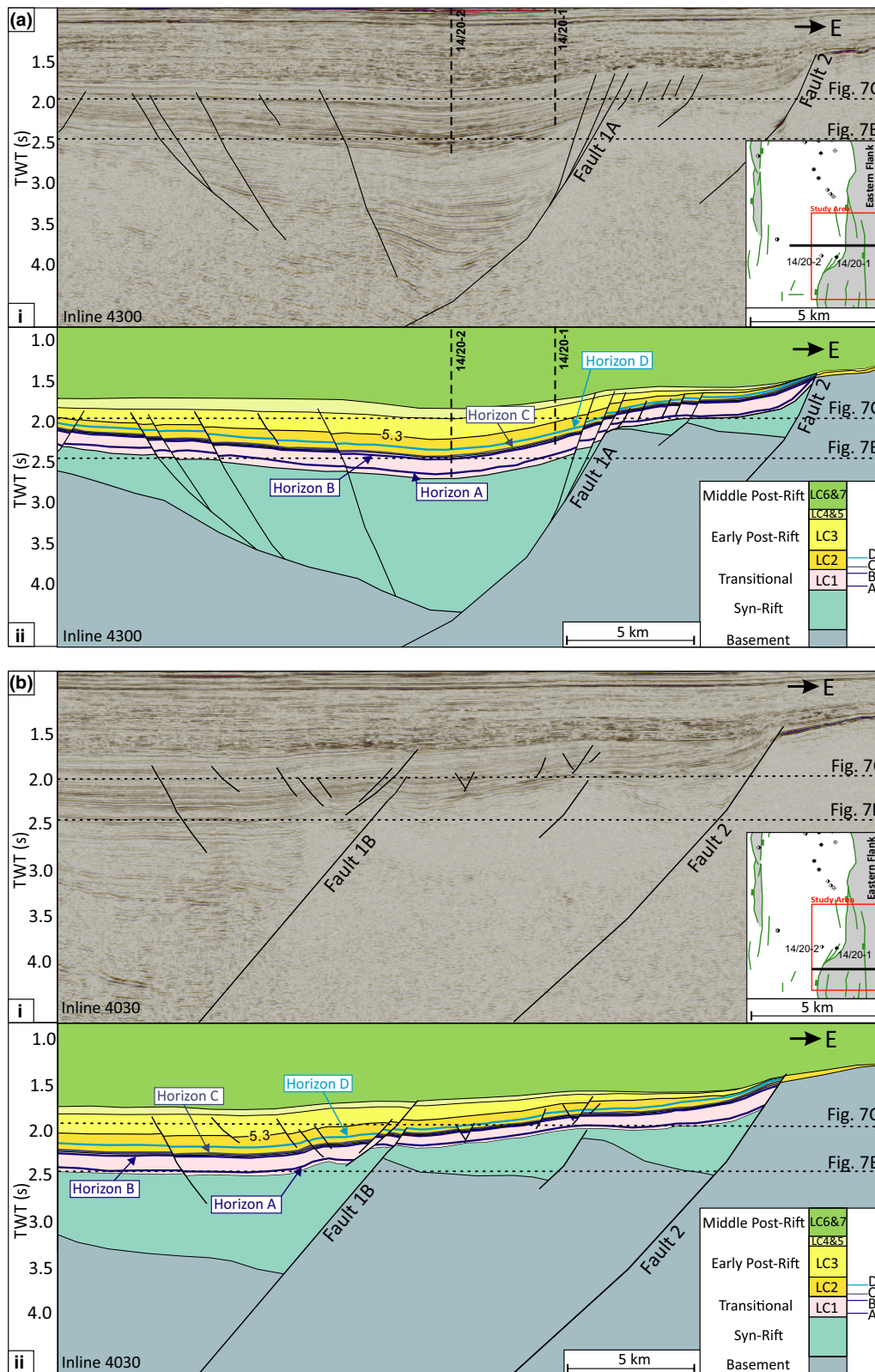


**FIGURE 8** Type cross-sections of the study area (a) i. Inline 4300 of the 3D company composite survey. ii. Geoseismic section of inline 4300 shows the asymmetric, fault controlled Eastern Graben and the smaller, fault controlled, asymmetric graben formed on the Sanson Terrace. Deep basement-involving faults are located at the basin margins and throughout the Eastern Graben, while shallow faults contained within the early post-rift interval are located on the Sanson Terrace. (b) i. Inline 4030 of the 3D company composite survey. ii. Geoseismic section of inline 4030 shows the Eastern Graben has shallowed to the south and the areal extent of the Sanson Terrace has extended to the west south of the fault bend. Major faulting is still focussed along basin margins and shallow faults on the Sanson Terrace are more sparse and of varied orientation

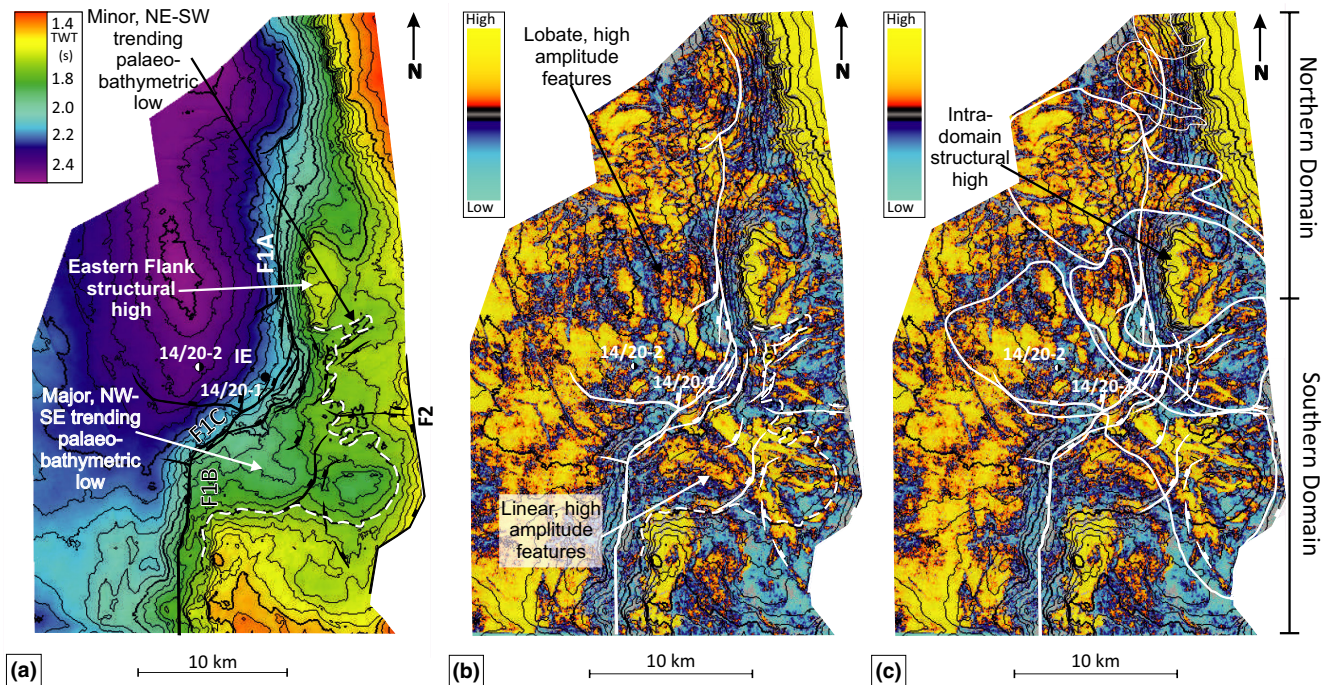


**FIGURE 9** Horizon A of the lower part of LC1. (a) Time-structure map shows the Eastern Graben and Sanson Terrace are separated by a large through-going fault and three distinct valley features across the Sanson Terrace. IE = Isobel Embayment. (b) RMS amplitude map generated from a 20 ms window of the horizon shows linear, high-amplitude geometries leading from palaeo-bathymetric lows on the Sanson Terrace, to lobate features in the Eastern Graben. (c) Interpreted depositional systems in the northern and southern domains. Systems enter the basin at structurally different points and with different feeder geometries. The intra-domain structural high can be seen to divert sedimentary routing pathways

Immediately north of this large topographic feature, there is a smaller (ca. 3 km wide) palaeo-bathymetric low that trends NE-SW towards the basin margin faults (Figure 9a).

The RMS amplitude map of the horizon shows a series of seismic architectures, possibly formed by two distinctly separate sedimentary systems (or 'domains'). Firstly, there is a generally linear, occasionally slightly sinuous series of high-amplitude features on the Sanson Terrace and in the Isobel Embayment (Figure 9b). These transition into more dispersed or lobate high-amplitude features observed extending off, and into the Eastern Graben. The area of linear features on the Sanson Terrace closely corresponds to areas of low topography (see dashed line on Figure 9a), the position of which occupies the fault bend/relay-ramp. Well 14/20-2 does not intersect any of the high-amplitude features in this southern domain; Horizon A is too deep for well 14/20-1 to intersect (Figure 9b). The GR response in well 14/20-2 does not indicate a significantly sandy response (Figure 5). The second domain occurs to the north and is characterised by a series of fan-shaped seismic amplitude geometries, which appear to branch outwards from a series of feeder systems. There are no wells in the location of the northern domain.

The two domains are separated by a structural high on the Eastern Flank (Figure 9a), which shows a relatively high-amplitude response (Figure 9b). An area of similar amplitude response is also present to the south of the relay-ramp, again over a structural high on TWTT maps, forming the southerly limits to the sinuous/straight seismic amplitudes (Figure 9b).

### Interpretation

The sinuous feeder systems, or channels, and associated fanning-outward lobate geometries indicate the presence of a series of diverse, deep-lacustrine fan systems at Horizon A. In the southern domain, the geometry of the high-amplitude responses contained within the palaeo-bathymetric lows indicate multiple sedimentary systems. Well 14/20-2 records a shaley GR response where it intersects the horizon at a low-amplitude response (Figure 5). These were fed through single or multiple canyons, which transported sediment from the Sanson Terrace down and into the deeper basin. The northern domain appears to compose a series of fans and depositional lobes that have a more line-sourced, or at least point-sourced character.

In the southern domain, the largest feeder system appears to be situated at the breached relay structure, in the

major NW-SE trending palaeo-bathymetric low. It crosses oblique to the overall basin margin, though perpendicular to Fault 1C, where it connects to depositional lobes in the Isobel Embayment and Easter Graben (Figure 9c). The smaller, NE-SW trending feeder system to the north appears to similarly connect across the basin margin to separate fan/lobe deposits in the Isobel Embayment (Figure 9c). The time structure expression of the NE-SW trending palaeo-bathymetric low suggests structural control or constraint of the feeder system observed within it. In comparison, the northern domain appears to be composed of generally smaller, outwards-fanning lobe geometries, which are more of point-sourced or line-sourced systems, especially in the northern part of the domain, and certainly compared with the systems in the southern domain. For the most part, the trajectory of both feeders, and depositional lobes is almost perpendicular to the basin margin-faults, with some more local scale variation, which is in stark contrast to the southerly domain that displays a dominant SE-NW trend. The two 'domains' appear to coalesce in the basin centre.

The 'intra-domain high' between the two sedimentary domains acts to separate the two domains along the basin margin (Figure 9c). Sedimentary systems immediately to the north and south of the structural high divert around it,

providing the key indication that it represented a positive palaeo-topographic feature at the basin margin during the time of deposition.

#### 4.2.2 | Horizon B

##### *Description*

Horizon B is contained within the upper part of LC1, closely underlying the top of the unit (Figure 8). Horizon B has experienced normal faulting by the basin margin faults and minor faults on the Sanson Terrace (Figure 10a). The Eastern Graben trends N-S along the faulted margin (Fault 1A), into Fault 1C at the Isobel Embayment (Figure 10a). The NW-SE trending palaeo-bathymetric low remains present on the Sanson Terrace and appears to have widened above the Isobel Embayment to approximately 12 km. The palaeo-bathymetric low contains NE-SW trending minor faults and appears to be bound by N-S trending minor faults to the north (Figure 10a). Further north on the Sanson Terrace, a smaller NE-SW trending palaeo-bathymetric low (<1 km wide), that was observed on Horizon A below (Figure 9a), is less prominent, as is the isolated high north of the low (Figure 10a).

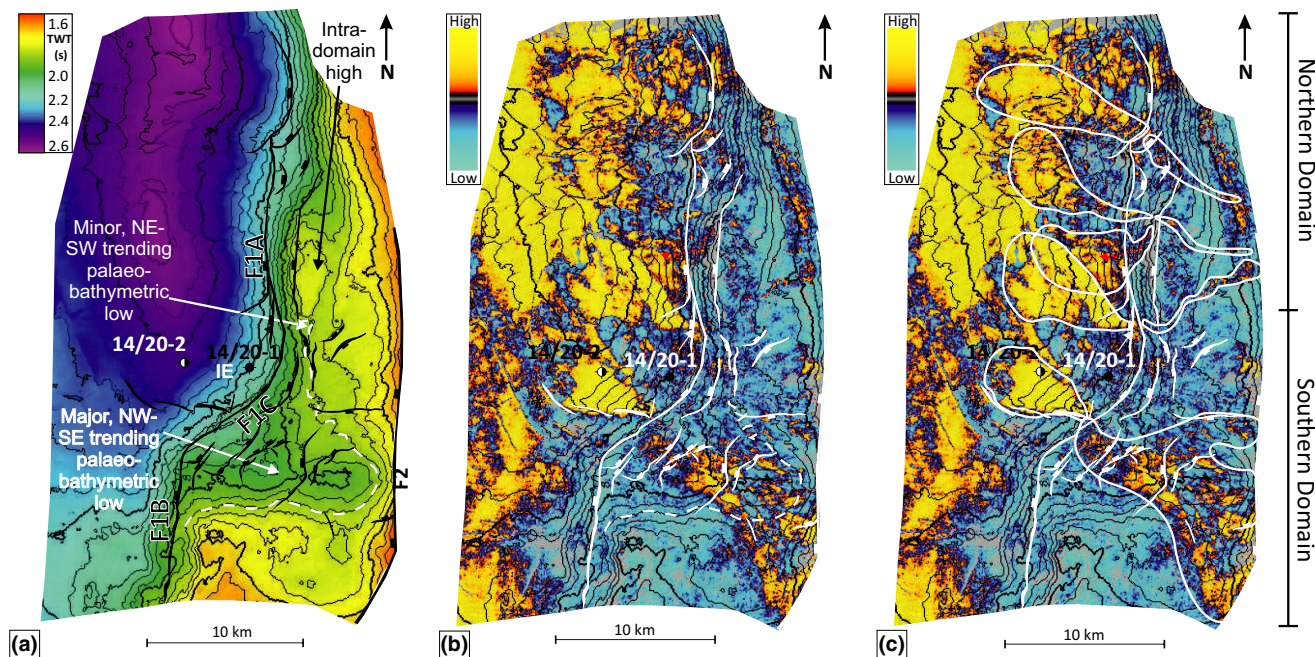


**FIGURE 10** Horizon B of the upper part of LC1. (a) Time-structure map shows the Sanson Terrace and its large valley, which remained a prominent paleo-topographic features towards the end of LC1. (b) RMS amplitude response of a 20 ms window, 10 ms above and below Horizon B, showing high-amplitude features within the palaeo-bathymetric low of the Sanson Terrace. Narrow zones of somewhat discontinuous high amplitudes are observed elsewhere on the terrace. (c) The northern domain is characterised by narrow, line-fed channels and associated down-flow depositional lobes in the Eastern Graben. The southern domain contains a larger feeder system comprised of a series of feeder channels that converge at the basin margin and deposit sediment as a fan in the Isobel Embayment. There are appears to be slight dextral offset on the southern domain system across Fault 1C

A series of linear and lobate, high-amplitude features are observed on the RMS amplitude map for this horizon. Linear geometries are focussed on the Sanson Terrace, while lobate geometries are present in the Eastern Graben (Figure 10b). There appear to be two distinct sedimentary domains with different seismic amplitude geometries observed between the north and the south of the study area (Figure 10b). To the south of the Sanson Terrace, a series of linear, high-amplitude features lie within the NW-SE trending palaeo-bathymetric low. The features lead from east of Fault 2, where they are widespread and appear to be in the hanging walls of minor faults, to Fault 1C where they have converged (Figure 10b). These linear, high-amplitude features then appear to disperse into a lobate geometry once across the basin margin (Fault 1C). Well 14/20-2 intersects the high-amplitude lobate feature (Figure 10b) and records a corresponding sandy GR response (Figure 5). Well 14/20-1 intersects the horizon at an area of low-amplitude response (Figure 10b), and GR response at this level indicates a shaley response (Figure 5).

In contrast, the northern extent of Sanson Terrace boasts relatively low-amplitude responses, except for narrow, short zones of linear high-amplitude features (Figure 10b). These limited, linear high-amplitude features commonly correspond to narrow palaeo-bathymetric lows, such as the NE-SW trending palaeo-bathymetric low observed in Figure 10a. The Eastern Graben contains a widespread high-amplitude response throughout much of its deeper extent. On the margin slopes, high amplitudes are patchier and appear to have a more linear geometry which connect the narrow palaeo-bathymetric lows on the Sanson Terrace to the more widespread high amplitudes deeper in the Eastern Graben (Figure 10b).

### *Interpretation*

In general, the high-amplitude, linear features and their transition to lobe geometries towards the Eastern Graben, could be interpreted as deep-lacustrine fans and their associated feeder systems in the Isobel Embayment on Horizon B (Figure 10c). In the southern domain, a significant sedimentary system, comprised of multiple feeder systems, which delivered sediment across the Sanson Terrace, is indicated by the sinuous high-amplitude features contained within the NW-SE palaeo-bathymetric low above the Isobel Embayment. In the southern domain there is a single feeder system within the NW-SE trending palaeo-bathymetric low, which occupies the area of the breached relay ramp. Up-dip on the Sanson Terrace, the feeder system appears to be contained and diverted by E-W and NW-SE trending minor faults. The feeder system narrows down-dip and converges above the Isobel Embayment. Across the margin slope, the feeder channels transition into lobate fan geometries, which are

deposited at the foot of the relay ramp (Figure 10c). There is a small dextral (ca. 1.5 km of lateral movement) offset between the feeder system on the Sanson Terrace and the deep-lacustrine fan in the Isobel Embayment across Fault 1C (Figure 10c). Wireline response for wells 14/20-1 and 14/20-2 indicate that the high-amplitude responses on this horizon may correspond to sand presence (Figure 5).

The northern domain is comprised of three point-sourced fan systems, indicated by narrow (<1 km wide), high-amplitude responses contained within narrow palaeo-bathymetric lows, which lead to high amplitudes on the margin slopes that then fan outwards into the deeper basin to the west (Figure 10c). These systems transport sediment from the Eastern Flank, down narrow channels, potentially confined in palaeo-bathymetric lows, across Fault 1A and subsequently form deep-lacustrine fans in the Eastern Graben, deposited directly adjacent to Fault 1A. The amplitude response within the narrow channels is patchier than the wider counterparts deposited in the NW-SE trending low of the southern domain; this may be due to seismic resolution issues or heterolithic channel fill (i.e. mud-filled channels across the slope; Figure 10c). The two southern-most channels (Figure 10c) display sinuous planform geometries and are deflected around the same intra-domain topographical high that separated the sedimentary domains of the underlying Horizon A. This high clearly had prolonged impact on the sedimentary systems entering from the Eastern Flank, and represents a key partitioning of the northern domain from that of the southern domain (Figures 9a and 10a). The most northerly point-sourced system appears to enter the basin at another, smaller-scale fault relay-ramp structure in Fault 1A (Figure 10c), highlighting the complex and fractal nature that is typical of these basin margin settings.

### 4.2.3 | Horizon C

#### *Description*

Horizon C overlies the base of LC2 (Figure 8). It shows offset by normal faulting along the basin margin, and minor normal faulting on the Sanson Terrace. The N-S trending Eastern Graben remains the main depocentre, extending from the Isobel Embayment north along Fault 1A (Figure 11a). On the Sanson Terrace, the NW-SE trending palaeo-bathymetric low, visible at Horizon B, remains prominent, though it has widened and its topography is slightly less steep sided than in Horizons A and B (Figure 11a). Its northern edge remains, bound by N-S trending normal faults. Additionally, NE-SW trending normal faults are contained within the palaeo-bathymetric low. To the north, the topography on the terrace is slightly less steep, and the narrow palaeo-bathymetric lows (such as the

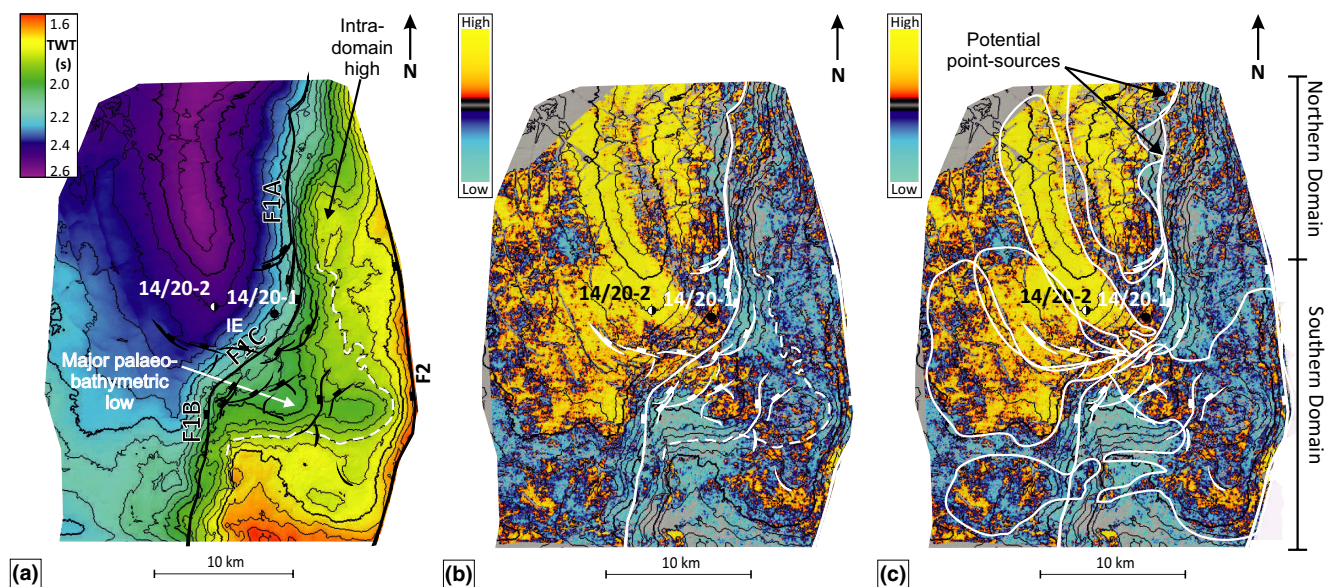


**FIGURE 11** Horizon C of LC2. (a) Time-structure map showing that the Sanson Terrace remained a palaeo-topographic high during LC2. The main palaeo-bathymetric low is also present, although it has widened basinwards compared with LC1 times. (b) RMS amplitude response of a 20 ms window, 10 ms above and below Horizon C, shows discontinuous high-amplitude architectures focussed within, and around, the main palaeo-bathymetric low on the Sanson Terrace, and widespread high amplitudes in the Eastern Graben. (c) Interpreted depositional systems show complex feeder geometries in the southern sedimentary domain, which transported sediment down into the main palaeo-bathymetric low and across the basin margin. These feeder geometries supplied sediment to numerous fans of differing geometries; perhaps controlled by the basin floor topography. The northern domain shows a scattered amplitude response indicating point sources or sub-seismic/poorly preserved feeders for the N-S trending, high-amplitude lobe, which is adjacent to Fault 1A

NE-SW trending low) are much less pronounced (Figure 10a).

The RMS amplitude response on the Sanson Terrace differs greatly from north to south, and continues to indicate the presence of separate sedimentary domains. The southern domain shows strong, linear, high-amplitude geometries, which align with the palaeo-bathymetric lows on the Sanson Terrace (Figure 11b). These linear, high-amplitude features appear to lead from the Eastern Flank, into the small palaeo-bathymetric low on the Terrace, and then branch in two different directions. Firstly, the brightest amplitudes are diverted into the main NW-SE trending palaeo-bathymetric low, and converge in the hanging wall of a NE-SW trending, basement-involving fault on the terrace. It then continues across Fault 1C and into the Isobel Embayment where the amplitude response appears to scatter and then transition into lobate features; the most significant of which is elongate and extends far into the basin (Figure 11b). The second branch is somewhat seismically dimmer, and composed of patchy, linear, high-amplitude features. These continue west, from the smaller palaeo-bathymetric low on the terrace towards Fault 1B. On meeting the basin margin, the weaker linear features remain patchy down the margin slope, eventually forming discontinuous lobate features on the basin floor (Figure

11b). Well 14/20-2 intersects the elongate high-amplitude feature (Figure 11b), which corresponds to a very faint sand response on the GR (Figure 5). Well 14/20-1 intersects an area of high amplitude, which fringes the high-amplitude feature (Figure 11b) and corresponds to a shaley GR response (Figure 5).

In the northern domain, discontinuous high amplitudes appear to correspond to palaeo-bathymetric lows on the Sanson Terrace (Figure 11b). These areas of high amplitude may lead to an E-W flowing, lobate, high-amplitude feature that lies in the Eastern Graben immediately adjacent to Fault 1A. The narrow NE-SW trending palaeo-bathymetric low, which lies to the north of the main NW-SE trending low, does not contain the same high-amplitude features as seen in Horizons A and B (Figure 11b). The lobe geometries appear to be sourced along a line corresponding to the strike of the northerly continuation of Fault 1B.

#### Interpretation

The high-amplitude, linear and lobate geometries described on Horizon C indicate the presence of deep-lacustrine fan systems sourced from the Sanson Terrace (Figure 11c). Like with previous horizons, both the northern and southern domains persist throughout this horizon.

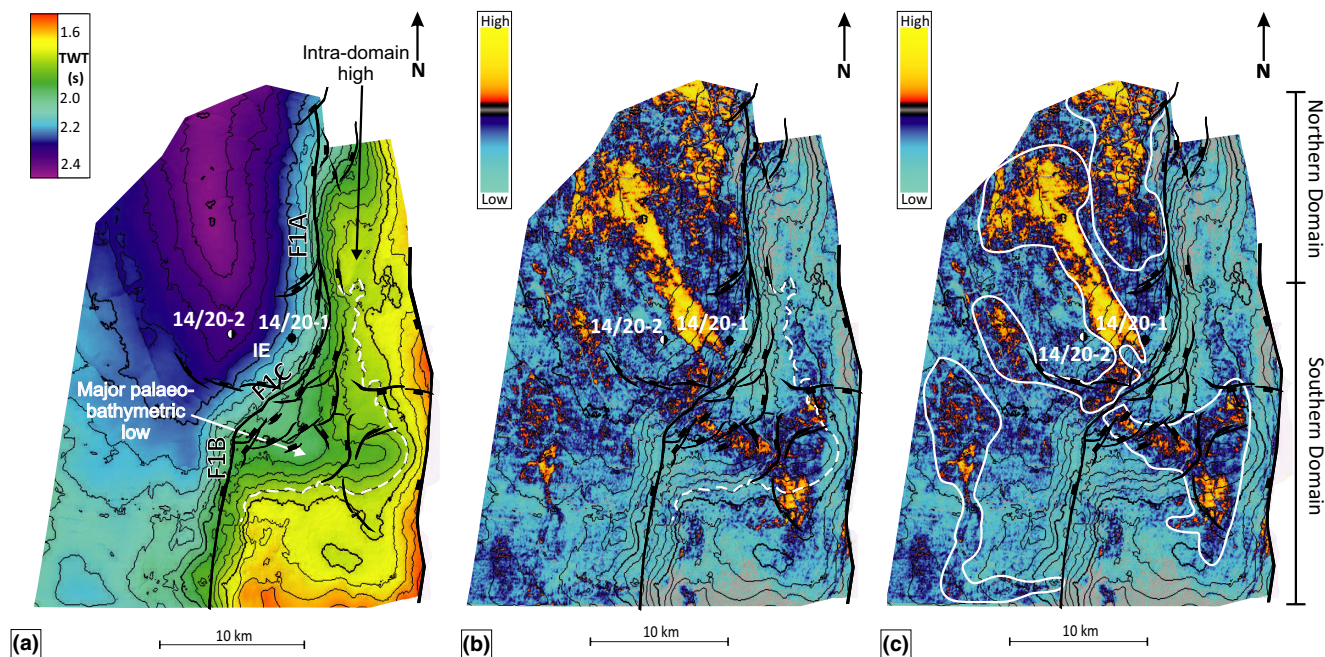


**FIGURE 12** Horizon D of LC2. (a) Time-structure map shows a gentler transitional slope, moving from the Sanson Terrace into the Eastern Graben, and the main palaeo-bathymetric low on the terrace remains a prominent feature. (b) RMS amplitude response of a 20 ms window, 10 ms above and below Horizon D, shows strong linear and lobate amplitude architectures within the palaeo-bathymetric low of the Sanson Terrace, and a high-amplitude elongate lobe in the depocentre maxima of the Eastern Graben. (c) An extensive sedimentary system in the southern domain, and a complex feeder system directed down the main palaeo-bathymetric low, with a change in probable flow direction occurring across the basin margin faults. The northern domain shows little amplitude response on the Sanson Terrace, and a N-S trending, discontinuous high-amplitude lobate feature on adjacent to Fault 1A

In the southern domain, an internally complex feeder system, which is concentrated in the main palaeo-bathymetric lows, supplies sediment to fans deposited in the Isobel Embayment, as well as a smaller fan deposited adjacent to Fault 1B (Figure 11c). The system deposited at the Isobel Embayment is likely fed by sediment shed from along the Eastern Flank, perhaps in the form of apron sands which hug the margin (indicated by discontinuous high amplitudes on the margin) and ponded sands that likely accumulated in the small palaeo-bathymetric low. This has led to sediment entering the main palaeo-bathymetric low from multiple directions where they appear to interact with and converge across a basement-involving, NE-SW trending fault on the terrace. This suggests that the smaller, basement-involving faults on the terrace have a significant impact on the geometry of the feeder systems. At the basin margin, sedimentary systems appear to disperse across the margin slope, and deliver sediment to a series of deep-lacustrine fans that extend out from the Isobel Embayment (Figure 11c).

The minor feeder system of the southern domain continues west from the area of ponded sediment in the southern domain and is significantly smaller than the major feeder system (Figure 11c). There are two linear channels that branch and trace west across the Sanson

Terrace, potentially diverted around a paleo-topographic high. The channels extend to Fault 1B, at which point they coalesce on the margin slopes and deposit a fan adjacent to Fault 1B, which has a discontinuous seismic response in plan-view (Figure 11c).

In the northern domain, a series of smaller fans are formed adjacent to Fault 1A. These systems are closely spaced and form as a line-sourced apron system, deposited directly adjacent to the fault structure. It is highly possible that the line-fed system was sourced locally from along the trace of the now likely rejuvenated Fault 1A structure. Indeed, the change in position of the fan system, orientation of fan geometries, and close spatial association with the trace of Fault 1A supports this interpretation. This is important as these observations would implicate fault reactivation and associated rejuvenation of the scarp associated with Fault 1A during this time. However, it is possible that they are fed by small-scale point sources that are below seismic resolution, or the features are backfilled with claystones. Discontinuous high-amplitude responses in palaeo-bathymetric lows may indicate sediment entry into the basin, although they do not suggest long-lived feeder systems (Figure 11c). There is uncertainty in the presence of line feeders for this domain as the RMS amplitude response does not show indicative zones of linear and

narrow high amplitudes contained in palaeo-bathymetric lows (Figure 11c); these features may be below seismic resolution or have been backfilled which would reduce the RMS amplitude response.

#### 4.2.4 | Horizon D

##### *Description*

Horizon D is contained within the LC2 sub-unit of the early post-rift interval (Figure 8). A gradual transitional slope separates the Sanson Terrace and the Eastern Graben, with minor (0.05 s) normal displacement on basin margin faults (Figure 12a). Minor faults on the Sanson Terrace offset this horizon by up to 0.02 s, with the majority trending NE-SW and contained within the NW-SE trending palaeo-bathymetric low (Figure 12a). The northern edge of the large, widened palaeo-bathymetric low does not appear to closely correspond to minor faulting at this level (Figure 12a). The topography of the Sanson Terrace is generally more gradual than observed at deeper horizons, rising to the south and east.

There is a significant difference in amplitude response between the north and south of the Sanson Terrace. On the south of the Sanson Terrace, there is a widespread, high-amplitude feature which corresponds with the major palaeo-bathymetric low, while the north of the terrace exhibits mostly low-amplitude response (Figure 12b). There may be two distinct sedimentary domains north and south on the terrace, or sedimentary systems may be concentrated in the southern extent of the terrace. The Eastern Graben has a generally low-amplitude response, with high amplitudes focused in elongate geometries in the deepest part of the basin and adjacent to Fault 1A (Figure 12b).

To the south of the Sanson Terrace, there are discontinuous and somewhat linear high amplitudes contained within the up-dip regions of the main NW-SE trending palaeo-bathymetric low. There appear to be two linear features in the up-dip region: a northerly one and a southerly one, which lead into the palaeo-bathymetric low and trend NE-SW and NW-SE, respectively. Down-dip of normal faults that cross the palaeo-bathymetric low, these two linear features converge and continue across the Sanson Terrace, further narrowing towards the top of the Isobel Embayment (Figure 12b). Across the basin margin faults, the feature appears to widen and lead to a large, elongate high-amplitude feature and a smaller, discontinuous lobate feature in the Eastern Graben (Figure 11b).

To the north, there is a consistently low-amplitude response across the Sanson Terrace, with no change in amplitude response corresponding with changes in topography (Figure 12b). Down-dip of Fault 1A there are patchy/discontinuous high-amplitude features, which appear to

spread down the margin slope and northwards from the low-amplitude area on the Sanson Terrace (Figure 12b).

##### *Interpretation*

Amplitude response in Horizon D indicates distinct northern and southern sedimentary domains. Domains are defined by generally low and limited, patchy high-amplitude responses in the north and contrasting high-amplitude features with widespread, distinct linear and lobate geometries in the south (Figure 12c). These contrasts suggest different source geometries and volumes of sediment transport and deposition were present in the domains. The southern domain appears to host a complex feeder system, which transports sediment from the Eastern Flank, across the Sanson Terrace, and down into the Isobel Embayment where the sediment is deposited as an elongate (>15 km) fan (Figure 12c). In the northern domain, there may be numerous point/sub-seismic linear sources that fed sediment directly over the hanging wall of Fault 1A to a patchy, loosely lobate feature in the basin (Figure 12c).

The southern domain contains an internally complex feeder system on the Sanson Terrace (Figure 12c). Sediment enters the system from the Eastern Flank, and is directed NE-SW and NW-SE down into the major palaeo-bathymetric low from two main locations (Figure 12c). There may be an element of sediment pooling at these two locations up-dip of the palaeo-bathymetric low, where contours indicate a relatively flat lying topography and there are strong, small, lobate, high-amplitude features (Figure 12c). This could suggest that a portion of the sediment shed from the Eastern Flank is gathered at these locations, which may then spill over and provide sediment to the feeder system (Figure 12c). Within the palaeo-bathymetric low, the NW-SE and NE-SW routes converge down-dip of a N-S trending, major fault which cross-cuts the valley, and the feeder system markedly narrows as a result (Figure 12c). The feeder then continues NW towards the basin margin, continuing to narrow as it does so. Sediment appears to spread across the faulted margin and down the margin slopes where it then feeds a large, elongate fan in the deepest part of the basin, and a smaller, patchy fan south of this (Figure 12c).

In the northern domain, a patchy fan deposited N-S on the hanging wall of Fault 1A can be traced up the margin slopes to the Sanson Terrace, indicating that there was likely a source situated on the Terrace (Figure 12c). There are no high-amplitude features observed on the Terrace at the location which would suggest the presence of a feeder system. This likely indicates a local, point source for the fan, which shed sediment straight down the Fault 1A hanging wall from the margin. Alternatively, there may be sub-seismic linear feeder

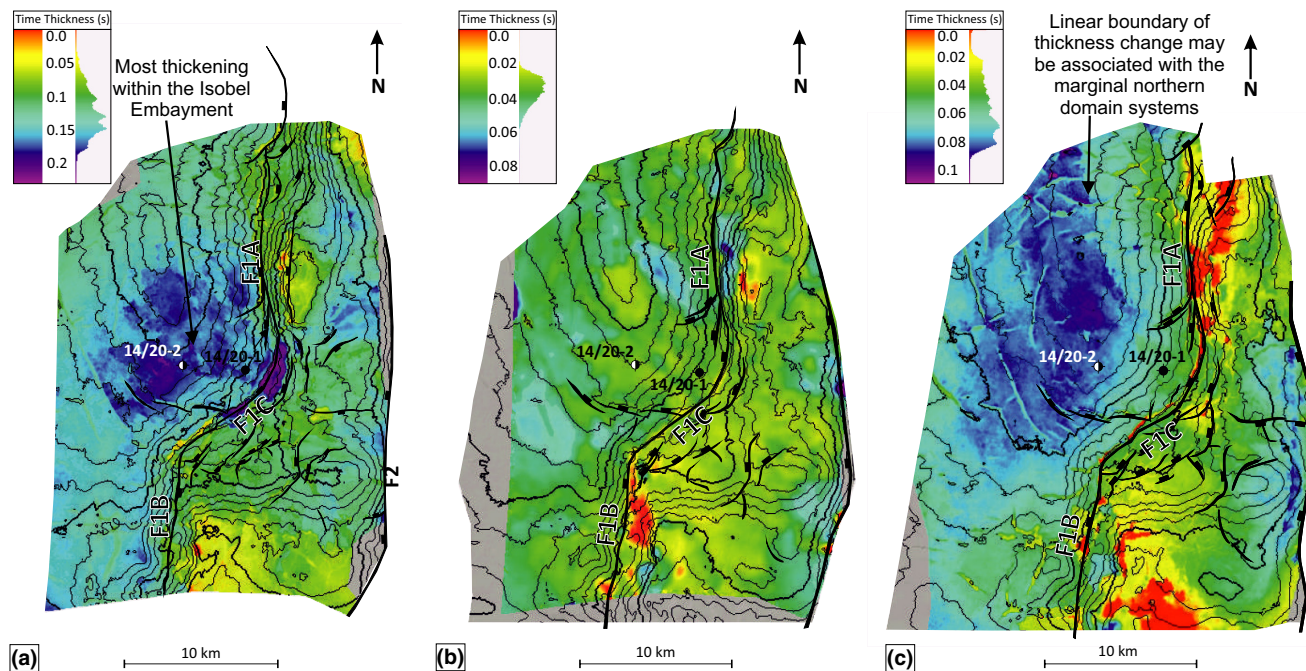


**FIGURE 13** Time thickness maps of the study horizon intervals. (a) Time thickness map of the A–B interval, with Horizon B structure contours overlain, showing clear thickening within the Isobel Embayment. The thickening appears to be contained by concentric faulting at the basin margin and into the Eastern Graben. This suggests that accommodation was still fault driven during LC1. (b) Time thickness map of the B–C interval, with Horizon C structure contours, showing a relatively widespread accumulation of around 0.04 s. Horizon C closely overlies Horizon B and this thin interval may prevent any trends in thickening being apparent. (c) Time thickness map of the C–D interval, with Horizon D structure contours, showing the most thickening of around 0.08 s in the centre of the basin. A linear change in thickness appears to run parallel to Fault 1A and may be an indication of the boundary between the Northern Domain fringing systems and the Southern Domain axial fans pushing out into the basin. Thickening in the centre of the basin likely indicates that accommodation space is driven by basin subsidence

systems, or such a system may have been eroded on the high. The northern domain system appears to have transported and deposited a much smaller volume of sediment than that which was brought into the basin by the southern domain system.

#### 4.2.5 | Time thickness analysis

##### *Description*

Time thickness maps of the intervals between Horizons A and B, B and C, and C and D, have been generated (Figure 13). The interval between Horizons A and B spans much of the transitional phase (Figure 13a). During this interval, maximum thickening of up to 0.2 s TWTT is contained in the Isobel Embayment and in the hanging walls of Fault 1C and others, which are synthetic to Fault 1C. On the Sanson Terrace, the most significant thickening (up to 0.15 s TWTT) occurs in the palaeo-bathymetric lows, while the interval thins onto the intra-domain structural high and the structural high in the south of the study area (Figure 13a).

The boundary between the transitional and early post-rift phase is contained within the interval between Horizon B and C. This interval is very thin, up to 0.01 s TWTT, and this may prevent thickness trends being readily apparent. Maximum thickening of up to 0.08 s TWTT lies in limited areas on the Sanson Terrace, specifically along Fault 2, and in the Eastern Graben (Figure 13b). The interval thins onto the intra-domain structural high and the structural high in the south of the study area.

The interval between Horizons C and D is contained within LC2 (Figure 13c). Maximum thickening, of up to 0.1 s TWTT, occurs in the centre of the Eastern Graben. In the basin centre, the eastern boundary of the area of maximum thickness cross-cuts contours and the interval appears to gradually thin up-dip towards Fault 1A. There are some limited patches of up to 0.1 s TWTT thickening on the Sanson Terrace, hugging Fault 2. Elsewhere on the Sanson Terrace, thickening (of up to 0.04 s TWTT) is contained within the palaeo-bathymetric lows, while the interval is dramatically thinner on the intra-domain structural high and the structural high in the south of the study area.

Interpretation

Accommodation space during the Horizons A to B interval (transitional phase) appears to have been fault driven as maximum thickening is contained within the Isobel Embayment and bounded by concentric faulting (Figure 13a). Although the B–C interval shows no strong trends in thickening, it does indicate that thickening is no longer focused within the Isobel Embayment or bounded by faulting (Figure 13b). This could suggest a cease/decrease in fault movement and associated accommodation space between the transitional phase and early post-rift (LC2). The C–D interval (early post-rift), shows that thickening is focused in the basin centre, suggesting that the main driver of accommodation space is basin subsidence by this time (Figure 13c). From the basin centre up-dip to Fault 1A, the thickness change is gradual and may indicate the presence of apron fans which were line-fed from Fault 1A and push out into the basin centre.

Time thickness maps indicate that the intra-domain structural high and southern structural high remained prominent throughout the study intervals as they are areas of consistent thinning (Figure 13). The southern structural high is likely associated with the upper portion of the breached relay ramp.

4.3 | Fan system geometries

Planform seismic high-amplitude features depicting a feeder system and associated lobe geometry are observed to coincide with sandstone deposits intersected in wells in the NFB, such as the Sea Lion, Casper and Beverley fans (Bunt, 2015; Dodd et al., 2019; Williams, 2015). As these fan systems and those in the Isobel Embayment (this study) are sourced from the same margin of the NFB and are deposited in broadly equivalent stratigraphy, this study draws on comparisons with these potentially highly analogous systems.

4.3.1 | Horizon A

There are two distinct sedimentary domains that input sediment at structurally contrasting locations on the basin margin (breached relay vs. hanging wall) and have different feeder geometries (dispersed/internally complex vs point/linear). The southern domain contains two sedimentary systems that enter the Eastern Graben at the breached relay location (Isobel Embayment) and are

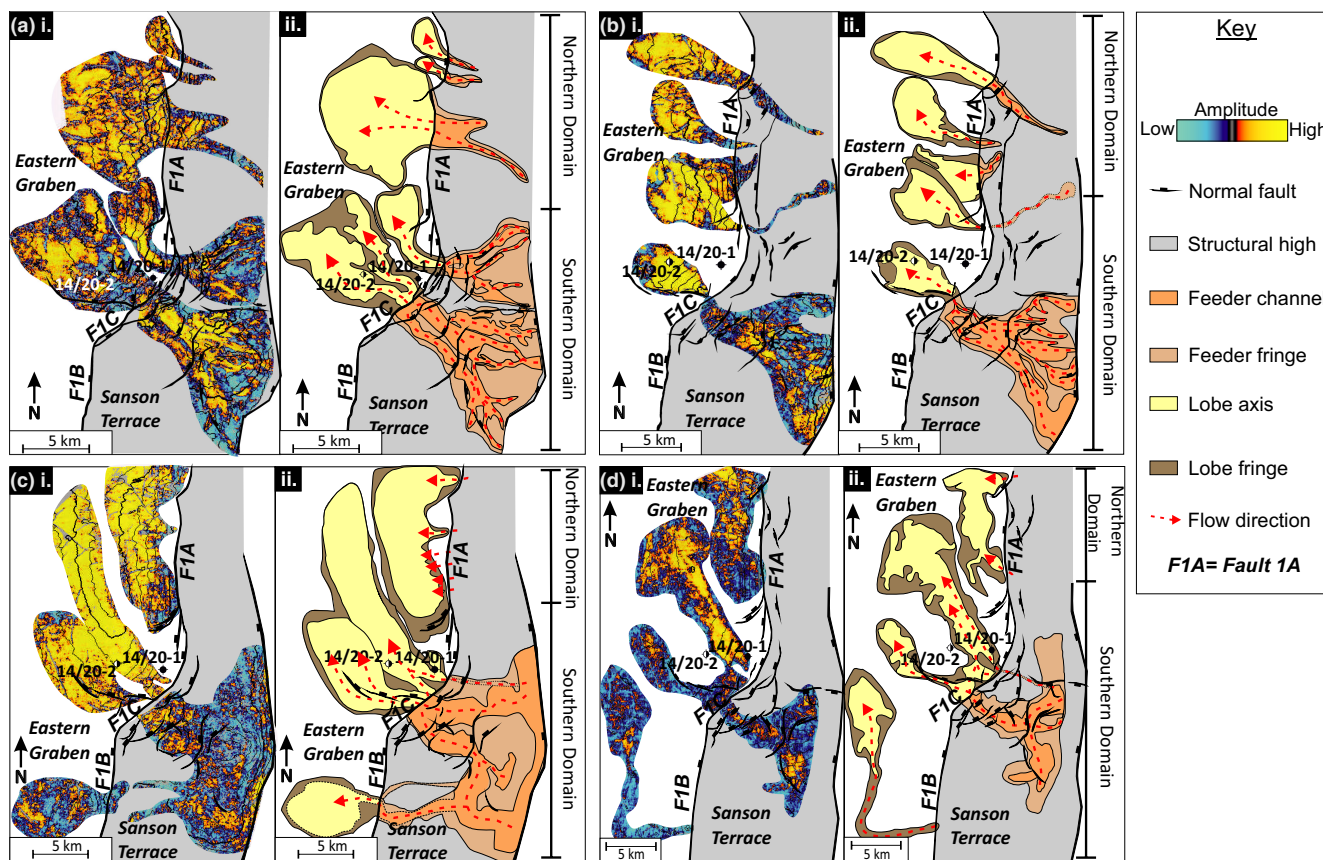


FIGURE 14 High-amplitude features observed on the study horizons (a.i to d.i) and their corresponding subaqueous sedimentary system interpretations (a.ii to d.ii). High-amplitude features enter the basin at the breached relay location or directly over Fault 1A (F1A)

derived from internally complex, sinuous feeder systems on the Sanson Terrace (Figure 14a). The northern domain shows numerous point or linear sourced systems of varying scale, entering the basin directly over the hanging wall of Fault 1A (Figure 14a).

The two large feeder systems in the southern domain are contained within palaeo-bathymetric lows on the Sanson Terrace. The larger and more-southerly of the two occupies the NW-SE palaeo-bathymetric low, entering the basin central and perpendicular to the NE-SW segment of the margin, spatially associated with the breached relay (Figure 14a). The smaller, more-northerly feeder system is contained within a smaller NE-SW trending palaeo-bathymetric low, which enters the basin at the northern limit of the NE-SW margin segment. In both systems, the up-dip regions are comprised of numerous sinuous and linear channels, which appear to converge down-dip of major sub-N-S trending faults that cross-cut the valleys (Figure 14a). Both systems further converge, approaching the basin margin and across the bounding faults, where they route down the slope and deposit as fans at the foot of the relay ramp (Figure 14a). At this level, there appears to be significant deposition in the up-dip regions of the systems, with widespread deposition across the Sanson Terrace. The fans deposited in the southern domain at Horizon A are patchy and somewhat limited laterally ranging from 4 to 7 km width (Figure 14a).

In comparison, simpler linear-fed fan systems characterise the northern domain. These feeders transported sediment directly down the hanging wall of Fault 1A, into the depocentre immediately adjacent to the fault segment. On the Sanson Terrace, the larger linear feeder leads from the Eastern Flank, is deflected north around a structural high, and then continues down the hanging wall slope (Figure 14a). These systems are associated with incised channels or canyons on the margin, possibly associated with residual footwall uplift. The northern domain systems terminate in lobate fans of varying scale, the largest is ca. 10 km in diameter, indicating the northern domain is important for sediment entry to the basin at this time.

Both northern and southern domains appear to result in fans of similar aerial extent, despite entering the basin at structurally different points on the margin. Although the fans appear comparable in size, the southern domain systems are likely larger, with sand trapped up-stream on the terrace. This could suggest that accommodation space created on the terrace, by further faulting and/or subsidence, has resulted in perched and dispersed feeder systems. The northern systems, by comparison, are much simpler with more confined feeders and isolated fans.

#### 4.3.2 | Horizon B

Both the southern and northern sedimentary domains persist at this level, defined by input at structurally different locations and contrasting feeder geometries on the margin. The southern domain contains a single fan and associated feeder system, entering the basin through the major palaeo-bathymetric low (Figure 14b). The feeder system appears to be widespread and internally complex, with numerous sinuous channels originating from the Eastern Flank and continuing down-slope into the palaeo-bathymetric low. These sinuous channels converge down-dip of a major, basement fault that cross-cuts the low and then continues to the basin margin. The system narrows across the basin margin and deposits a fan within the Isobel Embayment (Figure 14b).

The northern domain contains numerous sedimentary systems that deposit directly into the basin over the hanging wall of Fault 1A (Figure 14b). Many of these systems appear to originate from local point sources on the Sanson Terrace. A complex linear feeder has been interpreted to trace up to the Eastern Flank from the more southerly system, previously associated with the southern domain during the transitional phase. This feeder system is similar in character to those on the underlying Horizon A, with linear to mildly sinuous geometries, however it is acutely reduced in size and complexity (Figure 14a,b).

The northern domain systems appear to be more significant in both aerial extent and number of resultant fans. The southern system does have a larger and more widespread feeder system, which likely contains additional trapped, perched sands.

#### 4.3.3 | Horizon C

At Horizon C, sediment is input into the basin both at the breached relay location in the southern sedimentary domain, and directly across the hanging wall of Fault 1A in the northern sedimentary domain (Figure 14c). The southern sedimentary domain contains an internally complex feeder system on the Sanson Terrace, funnelling down through a canyon into the main palaeo-bathymetric low. The feeder system appears to emanate from two main areas, one in the south and the other in north along the easterly bounding fault of the Sanson Terrace (Figure 14cii). In addition to that, a westerly sediment route branches out from the main feeder system, perhaps as a result of overspill or a natural line of weakness associated with faults dissecting the relay, and deposits adjacent to Fault 1B as a patchy/discontinuous fan lobe (Figure 14c). However, the majority of sediment continues northwards into the main palaeo-bathymetric low. Here, the northern

and southern derived branches meet and converge down-dip of sub N–S faults that cross-cut the valley. Across the basin margin, this feeder system deposits two main fans; a lobate fan and an elongate fan (Figure 14c). The northern branch systems of the southern domain, particularly the fan closest to Fault 1A, are possibly laterally confined by the line-fed apron system of the northern domain. This has potentially encouraged the northern branch fans to become more elongate than the previously described systems of the southern domain. Additionally, reactivation of Fault 1A may have increased the lateral slope angle with which the southern domain fans interacted.

In contrast, the northern domain lacks laterally extensive feeder systems extending up and onto the Sanson Terrace. Despite this, there are numerous E–W-trending lobate fan geometries adjacent to Fault 1A. These fans were likely fed by local point sources on the margin (although sub-seismic linear sources on the terrace are not discounted). It is possible that extensive feeder systems are absent as a result of reduced preservation potential in the northern domain compared with the south. Alternatively, the lack of linear feeders on the Sanson Terrace at this level may be explained by footwall uplift and local sourcing of line-fed fan apron systems in down-dip locations. The fan apron systems are suspected to confine the southern domain fan systems, however, a paleo-topographic feature, such as a ridge, between the two could also have acted to separate and confine the two systems.

#### 4.3.4 | Horizon D

Like with the previous horizons, the sedimentary systems can be divided into northern and southern domains, although the southern domain is perhaps more-dominant by this point in time. The southern domain contains a number of elongate fans, which are fed by an internally complex feeder system focused within and up-dip of the main palaeo-bathymetric low on the Sanson Terrace (Figure 14d). The system is derived from the Eastern Flank, where sediment is input to the feeder system from two locations, north and south of the main palaeo-bathymetric low. The two end branches of the feeder system continue down-dip into the main palaeo-bathymetric low, converge down-dip of a sub N–S trending fault, and continue NW–SE towards the basin margin. On meeting the margin, the feeder swings to the NE, before depositing a northerly NW–SE-oriented elongate fan, along with a secondary subsidiary fan to the south (Figure 14d).

The northern domain contains two E–W-trending fans, down-dip of Fault 1B, with no clear corresponding feeder geometries on the Sanson Terrace (Figure 14d). The local point sources likely supplied sediment to the fans in the

hanging wall of Fault 1A and may have originated as a result of local rejuvenation of the escarpment. It is possible that there may be less input from point sources in the northern domain, with less sediment being delivered to the basin margin. Finally, the position of these fans, along with the linear NE edge of the elongate fans of the southern domain, may suggest lateral depositional confinement, with the two systems possibly baffling each other in the fan fringe areas. However, this same relationship is observed in the underlying Horizon C interval, and so it is also possible that pre-existing palaeo-topography in the basin centre (i.e. a ridge) acted to separate the two systems.

## 5 | DISCUSSION

This section examines the relationship between sedimentation and structure, and how a breached relay-ramp affected the formation of fans during the transitional and early post-rift phases. The influence of structure on fan feeder system routing, input loci (point sources) and plan-form character across the margin is evaluated. Resultant down-flow depositional fan characteristics, such as plan-form geometries and internal architectures, is explored. As a result, new insights into how partially covered, breached relay-ramps may influence sub-aqueous sediment gravity flow processes, as well as their effects on the spatial distribution of fan sandstones are provided.

### 5.1 | The relationship between structure and sedimentation

The relationship between sedimentation and structure is a well-known and widely documented aspect of deepwater sedimentary environments (e.g. Bell et al., 2018; Covault & Romans, 2009; Cullen et al., 2020; Cunha et al., 2017; Gervais et al., 2004; Lomas & Joseph, 2004; Prather et al., 1998; Tagliaferri et al., 2018; Winker, 1996). In complex settings, such as relay-ramps, structure has the potential to greatly influence sediment transport mechanisms and routing pathways (*sensu* Anderson et al., 2000; Athmer & Luthi, 2011; Barrett et al., 2020; Bruhn & Vagle, 2005; Serck & Braathen, 2019).

The observations and interpretations made in this study indicate an intimate relationship between sediment distribution and structure in breached relay settings, initially developing from the syn-rift surface, and being expressed throughout the transitional and early post-rift successions. To permit sufficient understanding in these settings, this study splits the relay ramp and structure-bounding fault hanging wall-associated sedimentary systems into different domains (termed ‘Northern’ and

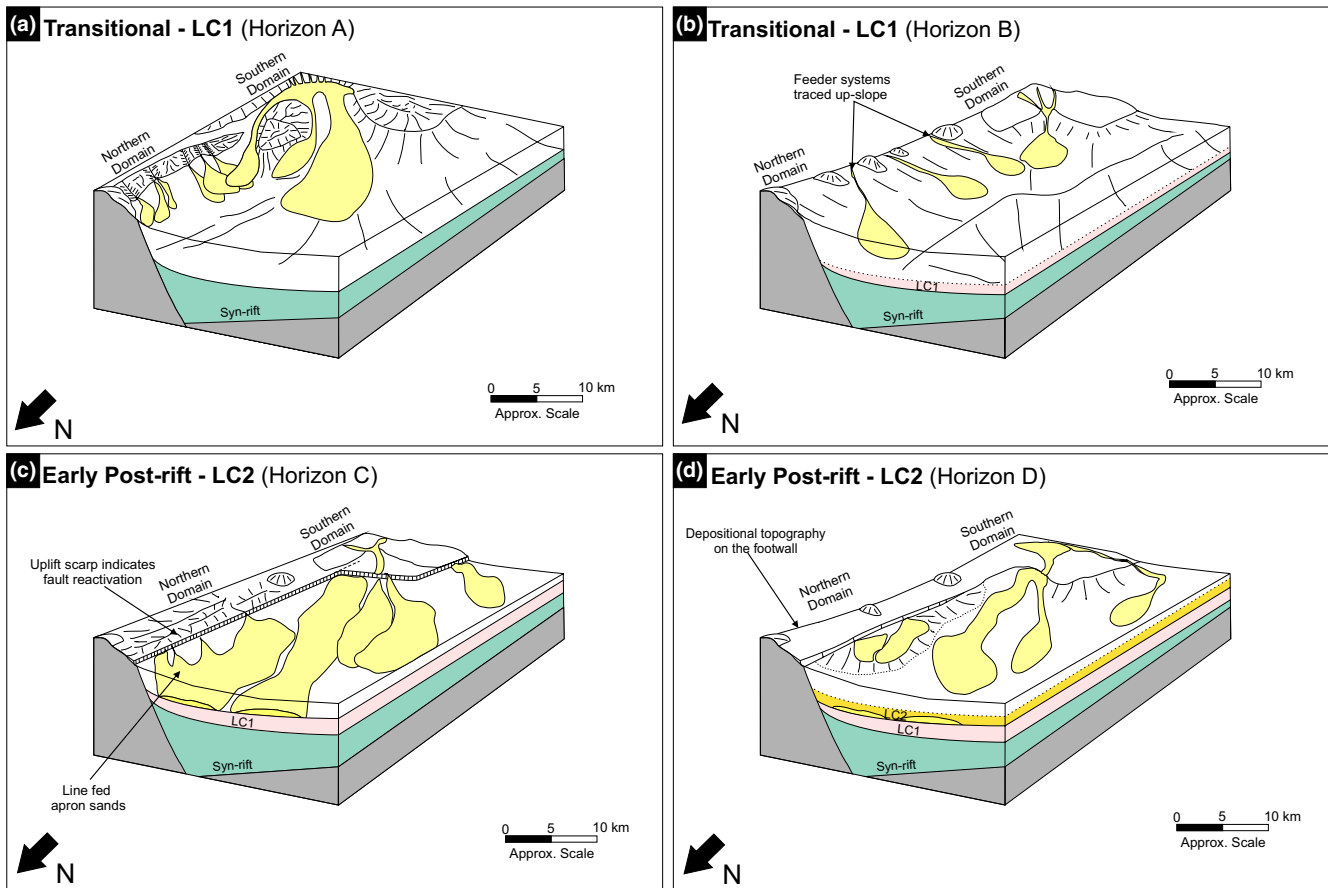


**FIGURE 15** 3D block models of the different transitional to early post-rift horizons (A–D). (a) LC1 sees significant sediment entry into the basin from the southern and northern domains. Fault escarpments are expected to be covered, creating a more sloped margin to the basin, allowing northern domain fans to be sourced from the Eastern Flank. Structural highs and lows strongly influence sediment pathways across the terrace and into the basin. (b) The later part of LC1 sees a possible reduction in sediment entry to the basin, with comparative deposition still occurring in both the northern and southern domains. Margins are more sloped as basin fill covers the fault structures below. (c) Fault reactivation has occurred between Horizon B and C, creating a defined fault escarpment at the basin margin. As a result, northern domain systems are locally sourced and line fed along the margin. Southern domain system continues to enter the basin through complex feeder systems, though the system appears more confined. This may be due to increased confinement associated with fault reactivation, subsidence and the line-fed apron systems of the northern domain. (d) The southern domain systems are more significant than the northern domain, line-fed systems, and continue to enter and deposit in a similar location. As the slopes reduce, some additional sediment pathways in the southern domain can form and sediment can leave the terrace to enter the basin across Fault 1B

‘Southern’ in this instance; Figure 14). These domains are defined by clear differences in sediment input location; associated fault structures; feeder system types and geometries; and resultant fan architectures. The fans within the northern domain remain largely perpendicular to the margin strike, deposited directly over the hanging wall of Fault 1A. They are point-sourced, largely by linear feeders that form across the slope during the intervals defined by Horizons A and B, before switching to more line-fed systems formed along Fault 1A during the intervals defined by Horizon C and D. The southern domain contains systems that consistently enter the basin in a more oblique orientation relative to the strike of Faults 1A and 1B, across the breaching fault on the relay ramp (Fault 1C).

These systems form smaller, lobate systems during the intervals defined by Horizons A and B, and then evolve into more elongate, slightly larger systems during the intervals defined by Horizons C and D. They are fed by complex, laterally widespread and diverse feeder systems entrenched within a key palaeo-bathymetric low on the Sanson Terrace. A few minor systems cross the Sanson Terrace and spill over into the hanging wall of Fault 1B (Figure 14c,d). These may be related to local faulting at the top of the ramp, which possibly formed in association with the breaching process, or may even be linked to fault re-activation. Indeed, there is evidence for the latter possibility elsewhere in the study area, namely the coeval input of line-source fans along Fault 1A in the Northern

Domain, and observed thickening into faults located across the terrace.

These two domains broadly correspond to published models that tend to highlight deposition occurring at either the base of the (non-breached) relay ramp, and/or adjacent to hanging wall faults (Athmer et al., 2010; Fugelli & Olsen, 2007; Ge et al., 2018). However, previous models (Athmer et al., 2010; Ge et al., 2018) suggest that the majority of deposition occurs across the hanging wall faults, whereas this study shows comparable sedimentary systems, in terms of scale and geometry, preserved in both the southern and northern domains (Figures 14 and 15). In fact, the southern domain appears to be fed by a more long-standing and diverse network of feeder systems preserved on the Sanson Terrace, highlighting the potential for basin margin terraces to trap sediments out of these settings, which will be largely dependent on accommodation space on the terrace. Comparatively, the northern domain systems, the analogue for hanging wall deposition, appear to diminish through time as the reactivation of basin bounding faults switch the source from distal to proximal along the fault length.

The wide palaeo-bathymetric low on the Sanson Terrace, located directly above the Isobel Embayment, is assumed to correspond to the location of the partially covered, subsided and breached lower ramp (Figure 7d). This feature remained present across all examples, though showed a gradual change from steeply dipping sides at Horizon A, to gently dipping slopes at Horizon D (Figures 9–12). This significant, and long-lasting, topographic feature served to direct sediment across the terrace, over the basin margin slopes, and into the Isobel Embayment. The complex feeder geometries entrenched within the palaeo-bathymetric low likely owe much of their genesis to this pre-existing lower ramp feature and potential pre-cut channels and/or canyons which may have developed before flooding, earlier in the basin's history.

The systems of the southern domain enter the basin at a very similar location on the Isobel Embayment (Figure 15), directed in through the Sanson Terrace palaeo-bathymetric low (Figure 14). The feeder systems in Horizon A and B are widespread and complex networks of diverse but largely sinuous to linear geometries. These gradually become more spatially constrained within the centre of the palaeo-bathymetric low, with fewer channels on the terrace during C and D times. It is quite possible that there is an association between the shifting feeder system locations and the evolving position of maximum offset along Fault 1C. Regardless, the development of the low above the breached lower ramp has served to direct these complex feeder systems into the Isobel Embayment for an extended period throughout the early post-rift.

The systems of the northern domain enter the basin over, and perpendicular to, the hanging wall of Fault 1A at reasonably consistent locations, although there is some variation through time (Figure 14). At Horizons A and B, the northern domain systems are comparative in shape (lobate), orientation (E–W trending) and size (10–15 km from proximal to distal). Most are point-sourced and fed by discrete channels that extend up or across the slope, eastwards and up-dip from Fault 1A (Figure 14). In comparison, sedimentary systems at Horizons C and D form more of a coalescing apron geometry, are individually much smaller in overall extent (ca. 5–7 km from proximal to distal), and were sourced from a more line-fed system along Fault 1A (Figure 14). It is likely that these changes reflect movement on Fault 1A, which must have occurred post-Horizon B (moving from LC1 into LC2), forming a positive feature and associated apron system by Horizon C (Figure 15). This is further supported by: (1) a coeval change in character of fan systems in the southern domain, with fan geometries being margin-restricted during Horizon A and Horizon B, after which they became more elongate, reaching further out into the basin (Figure 15); (2) the development of fan systems overspilling Fault 1B, possibly associated with further faulting and breaching of the ramp during later periods of fault movement.

Finally, the north-eastern edge of the system from the southern domain during Horizons C and D appear quite linear (particularly in D of Figure 14), possibly indicating some component, or at least influence, of small-scale confining topography on flows and/or overall fan morphology during this time. It is quite possible that an influencing intra-basinal palaeotopography was generated by the reactivation of around Fault 1A coupled with an actively building line-fed fan apron system on the lake floor.

In addition to the contrast between the southern and northern domains, there also appears to be significant differences between systems of the same domains deposited in the transitional (Horizons A and B) and the early post-rift (Horizons C and D) phases (Figures 13 and 14). Southern domain systems during the transitional phase consist of lobate fans confined to the Isobel Embayment (Figure 14a,b). Whereas the southern domain systems of the early post-rift (LC2) contain elongate fans which extend far beyond the Isobel Embayment (Figure 14c,d). These differences are likely associated with a change in accommodation space. Fault movement, particularly around the Isobel Embayment, is the main driver of accommodation space in the transitional phase, where the most significant thickening is clearly confined within the Isobel Embayment (Figure 13a). Into the early post-rift, fault movement has ceased (Figure 13b), and the most significant thickening becomes focussed in the basin

centre, suggesting that basin subsidence is the main driver of accommodation space at this point (Figure 13c). Additionally, the apron fans of the northern domain may have served to laterally confine the eastern edge of the southern domain fans, directing them further into the basin centre.

Northern domain systems of the transitional phase boast linear feeders across the terrace, which result in a number of lobate fans in the hanging wall of Fault 1A (Figure 14a,b). The northern domain systems of the early post-rift appear to be line-fed, without linear feeders, which bring sediment from across the Terrace, and result in apron-fans on Fault 1A (Figure 14c,d). Reactivation of Fault 1A between the transitional and early post-rift is the likely cause of change, as it would simultaneously shut off previously existing feeder channels by ways of footwall uplift and create a new source of sediment for the northern domain. Despite this potential reactivation of Fault 1A, the main driver of accommodation space at this time is overall basin subsidence (Figure 13c). This would suggest that the fault reactivation was short-lived and locally confined i.e. not a widespread or regional fault reactivation.

## 5.2 | The effect of buried breached relay ramps on subaqueous sediment gravity flows

Previous studies have addressed the effect of early-stage relay ramps in syn-rift settings on subaqueous sediment gravity flows (Anderson et al., 2000; Athmer & Luthi, 2011; Barrett et al., 2020; Bruhn & Vagel, 2005; Fugelli & Olsen, 2007; Ge et al., 2018; Soreghan et al., 1999). Early-stage relay ramps are observed to direct sediment down the ramp most effectively when there were pre-existing channels present on the ramp, the ramp had a landward tilt, or the direction of flow was oblique to the ramp orientation (as opposed to perpendicular; Ge et al., 2018). Although these factors lead to an increase in sediment volume directed down and deposited at the base of the ramp, significant portions of the flow volume were directed across and deposited at the base of hanging wall faults (Fugelli & Olsen, 2007; Ge et al., 2018). The examples presented in this paper offer insight into the effects of a breached relay ramp on transitional and early post-rift subaqueous sediment gravity flows.

The breached relay ramp of the study area (Figure 7) formed during active rifting and was progressively covered throughout the transitional to early post-rift phases (Figure 4). The palaeo-bathymetric low on the Sanson Terrace, likely associated with the covered, subsided and breached lower relay ramp, continuously directed

sediment into the basin at the Isobel Embayment. Although the breached relay had considerable sedimentary cover, the observations and interpretations of fan systems suggest a persistent influence over sedimentary routing during transitional and early post-rift times (Figures 1 and 15). The continued influence of margin structure over subaqueous sedimentary flows, after syn-rift tectonics ceased, indicates the retention of at least a subtle palaeo-topography (at a range of scales) throughout the transitional and early post-rift phases. This is possibly due to continued fault movement and structural influence during the transitional (Figure 13a) followed by overall basin subsidence driving accommodation space out in the basin (Figure 13c). This study indicates that localised extensional re-activation of a margin fault most-likely occurred between LC1 and LC2 (i.e. post-Horizon B and pre-Horizon C), indicated by major changes to sediment input location type and geometry, as well as overall contrasting fan architecture (described in-detail in earlier sections; Figure 15). General differential subsidence and/or compaction will have accounted for a component of accommodation space generation, but on its own is probably unable to explain the observed fundamental changes in the sedimentary systems that inhabited the margin. The appearance of line-fed apron systems along Fault 1A and over spilling fan systems across Fault 1B, both of which are present during Horizon C and D (Figure 15c,d), would be very challenging to explain through differential subsidence/compaction alone. The changes in fan geometry and sediment input through time (see block models in Figure 15), and the continued prevalence of northern and southern domains, suggests a persistent regional structure, both underlain and delineated by the breached-relay structure throughout the transitional and early post-rift of the NFB.

These examples show that relay ramp structures provide a strong influence on deepwater sedimentary systems formed within transitional and early post-rift successions, in rift basin settings. From this study, the following observations can be made: (1) the breached relay ramp fundamentally dictated the depositional topography at the end of the syn-rift, onto which the transitional and early post-rift units were deposited, and the flows of which interacted with; (2) the inherited topography and structural arrangement of the breached relay, in particular the abandoned lower ramp, consistently and preferentially directed transitional and early post-rift sub-aqueous sedimentary systems into the basin at the structure's location and (3) the breached relay ramp imparted a strong control on the orientation of fault re-activation and/or subsidence during later stages of basin fill, therefore influencing subsequent sedimentary systems deposited in the overburden.

### 5.3 | Implications for hydrocarbon exploration

Hydrocarbon exploration has generally focussed on syn-rift, deep-water turbidite reservoir rocks deposited in passive continental margins and rift basins (for example in the North Sea, Brazil and Africa; Destro et al., 2003; Evans, 1990; Genik, 1993; Guardado et al., 1989; Morely et al., 1990; Partington et al., 1993; Ravnås & Steel, 1997; Williams et al., 2020). Relay ramps, in particular, have long been locations of hydrocarbon exploration and prospectivity, as they are points of significant sediment entry into basins (Commins et al., 2005; Gawthorpe & Leeder, 2000; Gupta et al., 1999; Harding & Lowell, 1979; Leeder & Jackson, 1993; Lezzar et al., 2002; Morely, 1995; Morely et al., 1990; Nelson et al., 1992; Young et al., 2000; Williams et al., 2020). This study provides new insights into these complex settings, mainly using the well-imaged fan systems to detail, compare and contrast the potential distribution of reservoir fan sand in these settings, and in-particular how it evolves through time in response to changes in basin margin structure.

The northern sedimentary domain contains a diverse suite of systems that vary in feeder type, entry positions, and fan geometries through time (Figure 15). Structurally, the northern domain is dominated by Fault 1A, which appears to define the base of slope during Horizon A and B. As subaqueous sediment gravity flows, and more specifically turbidity currents, generally deposit coarse-grained material at the base of slopes, following a rheological jump (*sensu* Waltham, 2004 and references therein), it marks the eastward limit of lobe deposition, and therefore the majority of reservoir potential. Some potential may exist east of this line, but will be characterised by narrow, and geographically limited feeder systems that may contain volumes, but of low values. As discussed in earlier sections, Horizons C and D are marked by likely uplift of the footwall relative to the hanging wall, resulting in a series of slightly smaller-scale, line-fed fan apron systems deposited on the hanging wall side of the fault. The line source system is difficult to trace in a landward direction, and it is possible they were simply locally sourced from the emergent fault escarpment. The change in structural control, moving between Horizons B and C, resulted in a vertically and laterally complex suite of reservoirs, comprising potentially coarser-grained, poorly sorted, laterally limited fan apron deposits above, and finer-grained better sorted, laterally continuous fan sands below (*sensu* Richard & Bowman, 1998; Richard et al., 1998). The trapping geometries for the apron sands might be better, with abrupt terminations at Fault 1A. Stratigraphic trapping geometries at Horizons A and B are less favourable, with continuous feeder systems imaged up and onto the slope, resulting in

potential trap breaching (Figure 14). The close association with Fault 1B may promote hydrocarbon prospectivity, with relatively continuous fan deposition seemingly being associated with the position of the fault at all stratigraphic levels, leading to vertical aggradation of fan sandstone and potential for thickened pay in these settings. This is important to acknowledge, as these along-strike sites may be the less-liked cousin of the relay-ramp settings, in which explorers have historically concentrated efforts.

The southern domain consists of sedimentary systems that enter the basin at long-standing locations, which preserve vertically aggraded feeder systems over the Sanson Terrace (Figure 14). This might suggest reasonable hydrocarbon potential up on the terrace itself. In the basin centre, fans tend to either form as compensationally offset features, or are laterally offset from each other, making exploration drilling potentially costly. These fans tend to be more laterally extensive and reach further out into the basin centre, compared with those in the northern domain. Their larger geographical distribution may improve the in-place volumes within stratigraphic traps formed in these systems. Their longer transport distances may also promote hydrocarbon migration from the basinally located source kitchens, to the margin-located trapping geometries. However, there is also the possibility for stratigraphic sealing risks, with continuous feeder systems mapped up and onto the Sanson Terrace. Local fault sealing or sand-shale juxtaposition across basin margin faults, particularly Fault 1C, may offer closure to the down-dip located fan sandstone reservoirs.

Both the northern and southern domains see continuous sedimentary input from the margin and the Eastern Flank during the transitional and early post-rift. The southern domain is more consistent in feeder basin entry point, deposition locations and provenance, with some changes in fan shape through time. The northern domain systems are more variable, with smaller systems that shift slightly through time. They also have changing provenance, with switching from distal Eastern Flank sourcing to more local sources along the basin margin after periods of structural movement. The consistency and lateral extent of the southern domain systems make them more attractive for prospectivity; however, there is also potential for the northern domain systems to provide thick reservoir units, in well-defined trapping geometries.

## 6 | CONCLUSIONS

A breached relay-ramp characterises the structural arrangement at the Isobel Embayment; a site of major sediment transport, deposition and preservation along the Eastern margin of the NFB, during the Early Cretaceous.

The breached relay ramp clearly exerted a strong influence over the deep-lacustrine sedimentation from the transitional to early post-rift phases, affecting the routes of the sub-aqueous sediment gravity flows into the basin. Sediment was dominantly directed down a prominent palaeo-bathymetric low on the terrace, which is associated with the breached, subsided and covered lower ramp. This caused systems to consistently enter the basin at a similar position across Fault 1C and subsequently deposit in similar locations in the basin. This study shows that breached relays can be important sites of sedimentation in deep-lacustrine rift settings, with the potential for greatly variable sedimentary processes through time.

Additionally, a major fault associated with the breached relay appears to have been preferentially reactivated between the transitional and early post-rift phases (between LC1 and LC2). This is reflected in a change of source for the northern domain systems (distal to local) and resultant lobe shapes of the southern domain (rounded to elongate). This demonstrates the potential for breached relay ramp structures to exert renewed control on the spatial distribution and provenance of early post-rift sedimentary systems.

Two distinct sedimentary domains ('southern' and 'northern' within this study; termed 1 and 2, respectively) can be defined in the breached relay setting. These are characterised by differences in sediment input location, associated fault structures, feeder system types and geometries and resultant fan architectures. Domain 1 represents an area at the breached relay location and contains long-lived sedimentary systems with widespread feeder systems. Domain 2 represents the proximal basin-bounding faults and associated systems deposited directly over the hanging walls, which are generally smaller and more numerous with linear feeder systems. Both domains have similarities to previous syn-rift systems observed at earlier-stage relay ramps.

There is variable impact on sand distribution within the study area, between the breached relay site (southern domain) and across the hanging wall fault (northern domain). The southern domain sees consistent, laterally extensive lobes, which have been sourced from the Eastern Flank through widespread feeder systems. The northern domain systems contain small-scale lobes, which were deposited by small-scale feeders from the Eastern Flank or line sourced from along Fault 1A. They are more variable in size and sourcing.

## ACKNOWLEDGEMENT

We thank Xiaoyang Wu for his expertise and Romaine Graham for her thorough internal review. Tian Yang and Zhiyuan Ge are thanked for their insightful and helpful review comments, which significantly improved this

paper. We thank Peter Burgess for his editorial advice. The paper is published by permission of the Director, Mineral Resources, Falkland Islands Government and the Executive Director, British Geological Survey (UKRI).

## PEER REVIEW

The peer review history for this article is available at <https://publons.com/publon/10.1111/bre.12655>.

## DATA AVAILABILITY STATEMENT

The data that support the findings of this study are available from Falkland Islands Government Department of Mineral Resources. Restrictions apply to the availability of these data, which were used under license for this study. Data are available at <https://www.figuregov.fk/mineralresources/> with the permission of Falkland Islands Government.

## ORCID

Gayle E. Plenderleith  <https://orcid.org/0000-0002-2311-3863>

Thomas J. H. Dodd  <https://orcid.org/0000-0003-2257-6740>

## REFERENCES

- Anderson, J. E., Cartwright, J., Drysdall, S. J., & Vivian, N. (2000). Controls on turbidite sand deposition during gravity-driven extension of a passive margin: Examples from Miocene sediments in Block 4, Angola. *Marine and Petroleum Geology*, *17*, 1165–1203.
- Athmer, W., Groenenberg, R. M., Luthi, S. M., Donselaar, M. E., Sokoutis, D., & Willingshofer, E. (2010). Relay ramps as pathways for turbidity currents: A study combining analogue sandbox experiments and numerical flow simulations. *Sedimentology*, *57*(3), 806–823. <https://doi.org/10.1111/j.1365-3091.2009.01120.x>
- Athmer, W., & Luthi, S. M. (2011). The effect of relay ramps on sediment routes and deposition: A review. *Sedimentary Geology*, *242*(1–4), 1–17. <https://doi.org/10.1016/j.sedgeo.2011.10.002>
- Barrett, B. J., Hodgson, D. M., Jackson, C. A. L., Lloyd, C., Casagrande, J., & Collier, R. E. LI. (2020). Quantitative analysis of a footwall-scarp degradation complex and syn-rift stratigraphic architecture, Exmouth Plateau, NW Shelf, offshore Australia. *Basin Research*, *33*(2), 1135–1169.
- Bell, D., Stevenson, C. J., Kane, I. A., Hodgson, D. M., & Poyatos-Moré, M. (2018). Topographic controls on the development of contemporaneous but contrasting basin-floor depositional architectures. *Journal of Sedimentary Research*, *88*, 1166–1189. <https://doi.org/10.2110/jsr.2018.58>
- Bouma, A. H. (2000). Coarse-grained and fine-grained turbidite systems as end member models: Applicability and dangers. *Marine and Petroleum Geology*, *17*, 137–143. [https://doi.org/10.1016/S0264-8172\(99\)00020-3](https://doi.org/10.1016/S0264-8172(99)00020-3)
- Bowman, M. B. J. (1985). Cenozoic. In E. K. W. Glennie (Ed.), *Introduction to the petroleum geology of the North Sea*. JAPEC, Supplementary course notes no. 126.58. <https://doi.org/10.1002/9781444313413>

- Bruhn, R., & Vagle, K. (2005). Relay ramp evolution and mass flow deposition (Upper Kimmeridgian-Lower Volgian) in the tail end Graben, Danish North Sea. *Basin Research*, 17(4), 551–567. <https://doi.org/10.1111/j.1365-2117.2005.00276.x>
- Bunt, R. J. W. (2015). The use of seismic attributes for fan and reservoir definition in the Sea Lion Field, North Falkland Basin. *Petroleum Geoscience*, 21, 137–149. <https://doi.org/10.1144/petgeo2014-055>
- Carmona, A., Gratacós, O., Clavera-Gispert, R., Muñoz, J. A., & Hardy, S. (2016). Numerical modelling of syntectonic subaqueous sedimentation: The effect of normal faulting and a relay ramp on sediment dispersal. *Tectonophysics*, 684, 100–118. <https://doi.org/10.1016/j.tecto.2016.06.018>
- Childs, C., Watterson, J., & Walsh, J. J. (1995). Fault overlap zones within developing normal fault systems. *Journal of the Geological Society, London*, 152, 535–549. <https://doi.org/10.1144/gsjgs.152.3.0535>
- Çiftçi, N. B., & Bozkurt, E. (2007). Anomalous stress field and active breaching in relay ramps: A field example from Gediz Graben, SW Turkey. *Geological Magazine*, 144, 687–699.
- Commins, D., Gupta, S., & Cartwright, J. (2005). Deformed streams reveal growth and linkage of a normal fault array in the Canyonlands graben, Utah. *Geology*, 33(8), 645–648. <https://doi.org/10.1130/G21433AR.1>
- Covault, J. A., & Romans, B. W. (2009). Growth patterns of deep-sea fans, revisited Turbidite-system morphology in confined basins, examples from the California Borderland. *Marine Geology*, 265(1–2), 51–66. <https://doi.org/10.1016/j.margeo.2009.06.016>
- Cowie, P. A., Attal, M., Tucker, G. E., Whittaker, A. C., Naylor, M., Ganas, A., & Roberts, G. P. (2006). Investigating the surface process response to fault interaction and linkage using a numerical modelling approach. *Basin Research*, 18(3), 231–266. <https://doi.org/10.1111/j.1365-2117.2006.00298.x>
- Crossley, R. (1984). Controls of sedimentation in the Malawi rift valley, Central Africa. *Sedimentary Geology*, 40(1–3), 33–50. [https://doi.org/10.1016/0037-0738\(84\)90038-1](https://doi.org/10.1016/0037-0738(84)90038-1)
- Cullen, T. M., Collier, R. E. L. L., Gawthorpe, R. L., Hodgson, D. M., & Barrett, B. J. (2020). Axial and transverse deep-water sediment supply to syn-rift terraces: Insights from the West Xylokaastro Fault Block, Gulf of Corinth, Greece. *Basin Research*, 32(5), 1105–1139.
- Cunha, R. S., Tinterri, R., & Magalhaes, P. M. (2017). Annot Sandstone in the Peira Cava basin: An example of an asymmetric facies distribution in a confined turbidite system (SE France). *Marine and Petroleum Geology*, 87, 60–79.
- Destro, N., Szatmari, P., Alkmim, F. F., & Magnavita, L. P. (2003). Release faults, associated structures, and their control on petroleum trends in the Recôncavo rift, northeast Brazil. *AAPG Bulletin*, 87(7), 1123–1144. <https://doi.org/10.1306/02200300156>
- Dodd, T. J. H., McCarthy, D. J., & Richards, P. C. (2019). A depositional model for deep-lacustrine, partially confined, turbidite fans: Early Cretaceous, North Falkland Basin. *Sedimentology*, 66(1), 53–80. <https://doi.org/10.1111/sed.12483>
- Elliott, G. M., Jackson, C. A. L., Gawthorpe, R. L., Wilson, P., Sharp, I. R., & Michelsen, L. (2017). Late syn-rift evolution of the Vingleia Fault Complex, Halten Terrace, Offshore Mid-Norway: A test of rift basin tectono-stratigraphic models. *Basin Research*, 29(Suppl. 1), 465–487.
- Evans, A. L. (1990). Miocene sandstone provenance relations in the Gulf of Suez: Insights into synrift unroofing and uplift history. *AAPG Bulletin*, 74(9), 1386–1400.
- Fossen, H., & Rotevatn, A. (2015). Fault linkage and relay structures in extensional settings – A review. *Earth-Science Reviews*, 154, 14–28. <https://doi.org/10.1016/j.earscirev.2015.11.014>
- Frostick, L., & Reid, I. (1989). Is structure the main control of river drainage and sedimentation in rift? *Journal of African Earth Science*, 8(2–4), 165–182.
- Fugelli, E. M. G., & Olsen, T. R. (2007). Delineating confined slope turbidite systems offshore mid-Norway: The Cretaceous deep-marine Lysing Formation. *American Association of Petroleum Geologists Bulletin*, 91(11), 1577–1601. <https://doi.org/10.1306/07090706137>
- Gawthorpe, R. L., & Colella, A. (1990). Tectonic controls on coarse-grained delta depositional systems in right basins. Course grained deltas. <https://doi.org/10.1002/9781444303858>
- Gawthorpe, R. L., & Hurst, J. M. (1993). Transfer zones in extensional basins: Their structural style and influence on drainage development and stratigraphy. *Journal of the Geological Society (London)*, 150(6), 1137–1152. <https://doi.org/10.1144/gsjgs.150.6.1137>
- Gawthorpe, R. L., & Leeder, M. R. (2000). Tectono-sedimentary evolution of active extensional basins. *Basin Research*, 12, 195–218.
- Ge, Z., Nemeč, W., Gawthorpe, R. L., Rotevatn, A., & Hansen, E. W. M. (2018). Response of unconfined turbidity current to relay-ramp topography: Insights from process-based numerical modelling. *Basin Research*, 30(2), 321–343. <https://doi.org/10.1111/bre.12255>
- Genik, G. J. (1993). Petroleum geology of Cretaceous-Tertiary Rift Basins in Niger, Chad and Central African Republic. *AAPG Bulletin*, 77(8), 1405–1434.
- Gervais, A., Savove, B., Piper, D. J. W., Mulder, T., Cremer, M., & Pichevin, L. (2004). Present morphology and depositional architecture of a sandy confined submarine system: The Golo turbidite system (eastern margin of Corsica). *Geological Society of London Special Publications*, 222, 59–89. <https://doi.org/10.1144/GSL.SP.2004.222.01.05>
- Guardado, L. R., Gamboa, L. A. P., & Lucchesi, C. F. (1989). Petroleum geology of the Campos Basin, Brazil, a model for producing Atlantic type Basin: Part 1. In: J. D. Edwards, & P. A. Santogrossi (Eds.), *Divergent/passive margins*. *AAPG Memoir*, 48, 3–79.
- Gupta, S., Underhill, J. R., Sharp, I. R., & Gawthorpe, R. L. (1999). Role of fault interactions in controlling synrift sediment dispersal patterns: Miocene, Abu Alaqa Group, Suez Rift, Sinai, Egypt. *Basin Research*, 11(2), 167–189. <https://doi.org/10.1046/j.1365-2117.1999.00300.x>
- Harding, T. P., & Lowell, J. D. (1979). Structural styles, their plate tectonic habitats and hydrocarbon traps in petroleum provinces. *AAPG Bulletin*, 63(7), 1016–1058.
- Heller, P. L., & Dickinson, W. R. (1985). Submarine ramp facies model for delta-fed, sand-rich turbidite systems. *AAPG Bulletin*, 69(6), 960–976.
- Hemelsdaël, R., & Ford, M. (2016). Relay zone evolution: A history of repeated fault propagation and linkage, central Corinth rift, Greece. *Basin Research*, 28, 34–56. <https://doi.org/10.1111/bre.12101>
- Henstra, G. A., Grundvåg, S. A., Johannessen, E. P., Kristensen, T. B., Midtkandal, I., Nystuen, J. P., Rotevatn, A., Surlyk, F., Sæther, T., & Windelstad, J. (2016). Depositional processes and stratigraphic architecture within a coarse-grained rift-margin turbidite system: The Wollaston Forland Group, east Greenland.

- Marine and Petroleum Geology*, 76, 187–209. <https://doi.org/10.1016/j.marpetgeo.2016.05.018>
- Jackson, J., & Leeder, M. (1994). Drainage systems and the development of normal faults: An example from Pleasant Valley, Nevada. *Journal of Structural Geology*, 16(8), 1041–1059. [https://doi.org/10.1016/0191-8141\(94\)90051-5](https://doi.org/10.1016/0191-8141(94)90051-5)
- Kim, W., & Paola, C. (2007). Long-period cyclic sedimentation with constant tectonic forcing in an experimental relay ramp. *Geology*, 35, 331–334. <https://doi.org/10.1130/G23194A.1>
- Lambiase, J. J., & Bosworth, W. (1995). Structural controls on sedimentation in continental rifts. *Geological Society, London, Special Publications*, 80(1), 117–144.
- Leeder, M. R., & Gawthorpe, R. L. (1987). Sedimentary models for extensional tilt-block/half-graben basins. *Continental Extensional Tectonics. Geological Society Special Publications*, 28, 139–152. <https://doi.org/10.1144/GSL.SP.1987.028.01.11>
- Leeder, M. R., & Jackson, J. A. (1993). The interaction between normal faulting and drainage in active extensional basins, with examples from the western United States and central Greece. *Basin Research*, 5, 79–102. <https://doi.org/10.1111/j.1365-2117.1993.tb00059.x>
- Lezzar, K. E., Tiercelin, J. J., Le Turdu, C., Cohen, A. S., Reynolds, D. J., Le Gall, B., & Scholz, C. A. (2002). Control of normal fault interaction of major Neogene sedimentary depocentres, Lake Tanganyika, East African Rift. *AAPG Bulletin*, 86, 1027–1059.
- Lohr, T., & Underhill, J. R. (2015). Role of rift transection and punctuated subsidence in the development of the North Falkland Basin. *Petroleum Geoscience*, 21, 85–110. <https://doi.org/10.1144/petgeo2014-050>
- Lomas, S. A., & Joseph, P. (2004). Confined turbidite systems. *Geological Society London Special Publications*, 222, 1–7. <https://doi.org/10.1144/GSL.SP.2004.222.01.01>
- Morely, C. K. (1995). Developments in the structural geology of rifts over the last decade and their impact on hydrocarbon exploration. *Geological Society London Special Publications*, 80(1), 1–32.
- Morely, C. K., Nelson, R. A., Patton, T. L., & Munn, S. G. (1990). Transfer zones in the East Africa rift system and their relevance to hydrocarbon exploration in rifts. *AAPG Bulletin*, 74, 1234–1253.
- Mutti, E., & Normark, W. R. (1987). Comparing examples of modern and ancient turbidite systems: Problems and concepts. In J. K. Leggett, & G. G. Zuffa (Eds.), *Marine clastic sedimentology: Concepts and case studies* (pp. 1–38). Springer.
- Mutti, E., & Normark, W. R. (1991). An integrated approach to the study of turbidite systems. In P. Weimer, & M. H. Link (Eds.), *Seismic facies and sedimentary processes of submarine fans and turbidite systems* (pp. 75–106). Springer.
- Nelson, R. A., Patton, T. L., & Morely, C. K. (1992). Rift segment interaction and its relation to hydrocarbon exploration in rift systems. *AAPG Bulletin*, 76, 1153–1169.
- Partington, M. A., Mitchener, B. C., Milton, N. J., & Fraser, A. J. (1993). Genetic sequence stratigraphy for the North Sea Late Jurassic and Early Cretaceous: Distribution and prediction of Kimmeridgian-Late Ryazanian reservoirs in the North Sea and adjacent areas. In: J. R. Parker (Ed.), *Petroleum Geology of Northwest Europe: Proceedings of the 4th Conference* (pp. 347–370). Geological Society, London.
- Peacock, D. C. P., & Sanderson, D. J. (1991). Displacements, segment linkage and relay ramps in normal fault zones. *Journal of Structural Geology*, 13(6), 721–733. [https://doi.org/10.1016/0191-8141\(91\)90033-F](https://doi.org/10.1016/0191-8141(91)90033-F)
- Peacock, D. C. P., & Sanderson, D. J. (1994). Geometry and development of relay ramps in normal fault systems. *American Association of Petroleum Geologists Bulletin*, 78(2), 147–165.
- Prather, B. E., Booth, J. R., Steffens, G. S., & Craig, P. A. (1998). Classification, lithological calibration and stratigraphic succession to seismic facies of intraslope Basin, Deep-Water Gulf of Mexico. *AAPG Bulletin*, 82(5A), 701–728.
- Ravnås, R., & Steel, R. J. (1997). Contrasting styles of Late Jurassic syn-rift turbidite sedimentation: A comparative study of the Magnus and Oseberg areas, northern North Sea. *Marine and Petroleum Geology*, 14, 417–449.
- Richard, M., & Bowman, M. (1998). Submarine fans and related depositional systems II: Variability in reservoir architecture and wireline log character. *Marine and Petroleum Geology*, 15, 821–839. [https://doi.org/10.1016/S0264-8172\(98\)00042-7](https://doi.org/10.1016/S0264-8172(98)00042-7)
- Richard, M., Bowman, N., & Reading, H. (1998). Submarine-fan systems I: Characterization and stratigraphic prediction. *Marine and Petroleum Geology*, 16, 689–717. [https://doi.org/10.1016/S0264-8172\(98\)00036-1](https://doi.org/10.1016/S0264-8172(98)00036-1)
- Richards, P., Duncan, I., Phipps, C., Pickering, G., Grzywacz, J., Hoult, R., & Merritt, J. (2006). Exploring for fan and delta sandstones in the offshore Falklands Basins. *Journal of Petroleum Geology*, 29(3), 199–214. <https://doi.org/10.1111/j.1747-5457.2006.00199.x>
- Richards, P. C., & Fannin, N. G. T. (1997). Geology of the North Falkland Basin. *Journal of Petroleum Geology*, 20(2), 165–183. <https://doi.org/10.1111/j.1747-5457.1997.tb00771.x>
- Richards, P. C., Gatliff, R. W., Quinn, M. F., Williamson, J. P., & Fannin, N. G. T. (1996). The geological evolution of the Falkland Islands continental shelf. *Geological Society Special Publication*, 108(108), 105–128. <https://doi.org/10.1144/GSL.SP.1996.108.01.08>
- Richards, P. C., & Hillier, B. V. (2000a). Post-drilling analysis of the North Falkland Basin-Part 1: Tectono-stratigraphic framework. *Journal of Petroleum Geology*, 23(3), 253–272. <https://doi.org/10.1111/j.1747-5457.2000.tb01019.x>
- Richards, P. C., & Hillier, B. V. (2000b). Post-drilling analysis of the North Falkland Basin- Part 1: Petroleum system and future prospects. *Journal of Petroleum Geology*, 23(3), 253–272.
- Serck, C. S., & Braathen, A. (2019). Extensional fault and fold growth: Impact on accommodation evolution and sedimentary infill. *Basin Research*, 31(5), 967–990. <https://doi.org/10.1111/bre.12353>
- Soreghan, M. J., Scholz, C. A., & Wells, J. T. (1999). Coarse-grained, deep-water sedimentation along a border fault margin of Lake Malawi, Africa: Seismic stratigraphic analysis. *Journal of Sedimentary Research*, 69(4), 832–846. <https://doi.org/10.2110/jsr.69.832>
- Tagliaferri, A., Tinterri, R., Pontiggia, M., Da Pra, A., Davoli, G., & Bonamini, E. (2018). Basin-scale, high-resolution three-dimensional facies modelling of tectonically confined turbidites: An example from the Firenzuola system (Marnoso-arenacea Formation, northern Apennines, Italy). *AAPG Bulletin*, 102(8), 1601–1626.
- Talling, P. J. (2013). Hybrid submarine flows comprising turbidity current and cohesive debris flow: Deposits, theoretical and experimental analyses, and generalized models. *Geosphere*, 9(3), 460–488. <https://doi.org/10.1130/GES00793.1>

- Trudgill, B. D. (2002). Structural controls on drainage development in the Canyonlands grabens of southeast Utah. *AAPG Bulletin*, 86(6), 1095–1112.
- Walsh, J. J., Watterson, J., Bailey, W. R., & Childs, C. (1999). Fault relays, bends and branch-lines. *Journal of Structural Geology*, 21, 1019–1026. [https://doi.org/10.1016/S0191-8141\(99\)00026-7](https://doi.org/10.1016/S0191-8141(99)00026-7)
- Waltham, D. (2004). Flow transformation in particulate gravity currents. *Journal of Sedimentary Research*, 74(1), 129–134.
- Wells, J. T., Scholz, C. A., & Soreghan, M. J. (1999). Processes of sedimentation on a lacustrine border-fault margin: Interpretation of core from Lake Malawi, East Africa. *Journal of Sedimentary Research*, 69(4), 816–831.
- Williams, L. S. (2015). Sedimentology of the Lower Cretaceous reservoirs of the Sea Lion Field, North Falkland Basin. *Petroleum Geoscience*, 21, 183–198. <https://doi.org/10.1144/petgeo2014-039>
- Williams, R. M., Underhill, J. R., & Jamieson, R. J. (2020). The role of relay ramp evolution in governing sediment dispersal and petroleum prospectivity of syn-rift stratigraphic plays in the Northern North Sea. *Petroleum Geoscience*, 26(2), 232–246. <https://doi.org/10.1144/petgeo2019-096>
- Winker, C. D. (1996). High-resolution seismic stratigraphy of a Late Pleistocene submarine fan ponded by salt-withdrawal mini basins on the Gulf of Mexico continental slope. Offshore Technology Conference 8024, 6–9 (May 1996). Houston, TX, USA.
- Yang, T., Cao, Y., Liu, K., Tian, J., Zavala, C., & Wang, Y. (2020). Gravity-flow deposits caused by different initiation processes in a deep-lake system. *AAPG Bulletin*, 104(7), 1462–1499. <https://doi.org/10.1306/03172017081>
- Yang, T., Cao, Y., Liu, K., Wang, Y., Zavala, C., Friis, H., Song, M., Yuan, G., Liang, C., Xi, K., & Wang, J. (2019). Genesis and depositional model of subaqueous sedimentary gravity-flow deposits in a lacustrine rift basin as exemplified by the Eocene Shahejie Formation in the Jiyang Depression, Eastern China. *Marine and Petroleum Geology*, 102, 231–257.
- Young, M. J., Gawthorpe, R. L., & Sharp, I. R. (2000). Sedimentology and sequence stratigraphy of a transfer zone coarse-grained delta, Miocene Suez Rift, Egypt. *Sedimentology*, 47(6), 1081–1104. <https://doi.org/10.1046/j.1365-3091.2000.00342.x>
- Zhang, C., Sholz, C. A., & Harris, A. D. (2020). Sedimentary fills and sensitivity analysis of deep lacustrine facies in multi-segment rift basins: Insights from 3D forward modelling. *Sedimentary Geology*, 408, 105753.
- Zhang, X., & Sholz, C. A. (2015). Turbidite systems of lacustrine rift basins: Examples from the Lake Kivu and Lake Albert rifts, East Africa. *Sedimentary Geology*, 325, 177–191. <https://doi.org/10.1016/j.sedgeo.2015.06.003>

**How to cite this article:** Plenderleith, G. E., Dodd, T. J. H., & McCarthy, D. J. (2022). The effect of breached relay ramp structures on deep-lacustrine sedimentary systems. *Basin Research*, 34, 1191–1219. <https://doi.org/10.1111/bre.12655>